NeuroImage 156 (2017) 315–339

Contents lists available at ScienceDirect

NeuroImage

journal homepage: www.elsevier.com/locate/neuroimage

Normative morphometric data for cerebral cortical areas over the lifetime of the adult human brain

Olivier Potvin[a], Louis Dieumegarde[a], Simon Duchesne[a,b,*], for the Alzheimer's Disease Neuroimaging Initiative[1]

[a] Centre de recherche CERVO Research Center, 2601, de la Canardière, Québec, Canada G1J 2G3
[b] Département de radiologie, Faculté de médecine, Université Laval, 1050, avenue de la Médecine, Québec, Canada G1V 0A6

ARTICLE INFO

Key words:
magnetic resonance imaging
atrophy
morphometry
normality
aging
sex

ABSTRACT

Proper normative data of anatomical measurements of cortical regions, allowing to quantify brain abnormalities, are lacking. We developed norms for regional cortical surface areas, thicknesses, and volumes based on cross-sectional MRI scans from 2713 healthy individuals aged 18 to 94 years using 23 samples provided by 21 independent research groups. The segmentation was conducted using *FreeSurfer*, a widely used and freely available automated segmentation software. Models predicting regional cortical estimates of each hemisphere were produced using age, sex, estimated total intracranial volume (eTIV), scanner manufacturer, magnetic field strength, and interactions as predictors. The explained variance for the left/right cortex was 76%/76% for surface area, 43%/42% for thickness, and 80%/80% for volume. The mean explained variance for all regions was 41% for surface areas, 27% for thicknesses, and 46% for volumes. Age, sex and eTIV predicted most of the explained variance for surface areas and volumes while age was the main predictors for thicknesses. Scanner characteristics generally predicted a limited amount of variance, but this effect was stronger for thicknesses than surface areas and volumes. For new individuals, estimates of their expected surface area, thickness and volume based on their characteristics and the scanner characteristics can be obtained using the derived formulas, as well as Z score effect sizes denoting the extent of the deviation from the normative sample. Models predicting normative values were validated in independent samples of healthy adults, showing satisfactory validation R^2. Deviations from the normative sample were measured in individuals with mild Alzheimer's disease and schizophrenia and expected patterns of deviations were observed.

Introduction

Several neuropsychiatric and neurological disorders are well known to yield distinctive cortical changes as measured by anatomical magnetic resonance imaging (MRI); such is the case, for example in Alzheimer's disease (AD) and schizophrenia (SZ; Bakkour et al., 2009; Haijma et al., 2013). However, one difficulty to determine whether an individual displays significant cortical variations of potential pathological origin is the lack of proper normative values, allowing to quantify the extent of the deviation from the normality of a given individual, adjusted for personal characteristics. Indeed, cortical measures are substantially influenced by various factors including sociodemographic factors, such as age and sex (Fjell et al., 2009; Pfefferbaum et al., 2013; Sowell et al., 2007; Storsve et al., 2014; Thambisetty et al., 2010; Walhovd et al., 2011) as well as total intracranial volume (Barnes et al., 2010; Crivello et al., 2014).

Very few attempts have been proposed to produce neuromorphometric normative values (Kruggel, 2006; Walhovd et al., 2011), stemming from the fact that three major hurdles needed to be overcome. The first is the requirement to use automated segmentation procedures, in order for measurements to be replicable. The second is to use a large sample of individuals, since sufficient representability is needed over a wide age range. The third is the necessity to incorporate data from multiple scanner configurations in order to allow the normative values to be usable for most researchers, as these characteristics (e.g. manufacturer and magnetic field strength) have an effect on the measurements (Govindarajan et al., 2014; Han et al., 2006; Kruggel et al., 2010; Potvin et al., 2016b).

* Correspondence to: Centre de recherche CERVO Research Center, F-3582, 2601, de la Canardière, Québec, Canada G1J 2G3.
E-mail address: simon.duchesne@fmed.ulaval.ca (S. Duchesne).

[1] Part of the data used in this article were obtained from the Alzheimer's Disease Neuroimaging Initiative (ADNI) database (adni.loni.usc.edu). As such, the investigators within the ADNI contributed to the design and implementation of ADNI and/or provided data but did not participate in analysis or writing of this report. A complete listing of ADNI investigators can be found at: http://adni.loni.usc.edu/wp-content/uploads/how_to_apply/ADNI_Acknowledgement_List.pdf.

http://dx.doi.org/10.1016/j.neuroimage.2017.05.019
Received 7 March 2017; Received in revised form 3 May 2017; Accepted 11 May 2017
Available online 13 May 2017

Table 1
Participants' characteristics according to the dataset.

Dataset	n	%	Age (mean ± SD range)	Female %
1. Autism Brain Imaging Data Exchange (ABIDE)	184	6.8	26.1 ± 7.0 18–56	12.5
2. Alzheimer's Disease Neuroimaging Initiative (ADNI1)	199	7.3	75.7 ± 5.0 60–90	47.2
3. Alzheimer's Disease Neuroimaging Initiative (ADNI2)	179	6.6	73.6 ± 6.3 56–89	52.5
4. Australian Imaging Biomarkers and Lifestyle flagship study of ageing (AIBL)	158	5.8	72.1 ± 7.2 60–88	52.5
5. BMB - Berlin Mind and Brain (Margulies, Villringer) CoRR sample (BMB)	50	1.8	30.3 ± 7.1 19–59	52.0
6. Cleveland Clinic (Cleveland CCF)	30	1.1	43.1 ± 11.1 24–60	63.3
7. Center of Biomedical Research Excellence (COBRE)	71	2.6	35.5 ± 11.3 18–62	29.6
8. DS-108 from the OpenfMRI database	32	1.2	22.2 ± 4.6 18–41	50.0
9. DS-170 from the OpenfMRI database	15	0.6	25.4 ± 4.6 19–35	20.0
10. Functional Biomedical Informatics Research Network (FBIRN)	34	1.3	38.9 ± 13.1 19–65	41.2
11. FIND lab sample (FIND)	13	0.5	24.1 ± 3.7 18–29	61.5
12. International Consortium for Brain Mapping (ICBM)	148	5.5	25.0 ± 4.9 18–44	43.2
13. Information eXtraction from Images (IXI)	558	20.5	48.5 ± 16.4 20–86	55.7
14. F.M. Kirby Research Center neuroimaging reproducibility data (KIRBY-21)	20	0.7	31.9 ± 9.7 22–61	45.0
15. Minimal Interval Resonance Imaging in Alzheimer's Disease (MIRIAD)	21	0.8	69.8 ± 7.5 58–86	47.8
16. NIH MRI Study of Normal Brain Development (NIHPD)	59	2.2	18.9 ± 1.0 18–22	52.4
17. Nathan Kline Institute Rockland phase 1 (NKI-R1)	138	5.1	42.4 ± 18.3 18–85	43.5
18. Nathan Kline Institute Rockland phase 2 (NKI-R2)	253	9.3	46.1 ± 18.8 18–85	64.8
19. Open Access Series of Imaging Studies (OASIS)	301	11.1	43.9 ± 23.6 18–94	61.8
20. POWER Neuroimage sample (POWER)	26	1.0	23.0 ± 1.4 20–25	84.6
21. Parkinson's Progression Markers Initiative (PPMI)	164	6.0	60.1 ± 11.5 31–83	34.2
22. TRAIN-39 sample (TRAIN)	35	1.3	22.5 ± 2.6 18–28	71.4
23. University of Wisconsin (Birn, Prabhakaran, Meyerand) CoRR sample (UWM)	25	0.9	25.0 ± 3.2 21–32	44.0
Total	**2713**	**100.0**	**47.6 ± 21.7 18–94**	**49.8**

We recently published such normative data fulfilling these requirements for subcortical regional volumes (Potvin et al., 2016a, b). We employed *FreeSurfer*, a freely available automated segmentation software widely used in the neuroscience community (Fischl, 2012). Using the same methodology, the present study aimed to produce normative data for cortical gray matter in terms of regional surface areas, thicknesses, and volumes according to age, sex and estimated intracranial volume (eTIV) while taking into account scanner manufacturer and magnetic field strength (MFS).

Materials and methods

Normative sample

We assembled a sample of 3D T1-weighted MRI scans from 2757 cognitively healthy controls aged 18 to 94 years by federating 23 samples provided by 21 independent research groups (see Table 1 and Acknowledgments for details). Of note, this includes the *Alzheimer's Disease Neuroimaging Initiative* (ADNI) and the *Australian Imaging, Biomarkers and Lifestyle study of aging* (AIBL) databases. The ADNI (adni.loni.usc.edu) was launched in 2003 as a public-private partnership, led by Principal Investigator Michael W. Weiner, MD. (www.adni-info.org). The AIBL data was collected by the AIBL study group and AIBL study methodology has been reported previously by Ellis et al. (2009). Scans were acquired from one of the three leading manufacturers (e.g. Siemens Healthcare, Philips Medical Systems, or GE Healthcare) at MFS of either 1.5 or 3T. For each dataset, approval from the local ethics board and informed consent of the participants were obtained.

All samples specifically recruited healthy control participants, except NKI1 and NKI2. Databases with older adults excluded neurological diseases and neuropsychiatric disorders with extensive assessments for age-related disorders. For databases recruiting in the general population (NKI1 and NKI2), we excluded participants with schizophrenia or other psychotic disorders, bipolar disorders, major depressive disorders and substance abuse/dependence disorders. Additional exclusions were made for NKI2: neurodegenerative and neurological disorders, head injury with loss of consciousness/amnesia, and lead

Table 2
Scanners, sequence, and participants characteristics.

Manufacturer	Magnetic field strength (%)	Voxel size in mm^3 (%)	Acquisition plane (%)	Model (%)	Age (mean ± SD) Range	Sex
GE	**1.5T** (52.9)	0.4 (4.6) 1.0 (7.6) 1.1 (64.0) 1.2 (3.0) 1.3 (13.2) 1.4 (7.6) Unknown (1.0)	Axial (28.1) Coronal (10.6) Sagittal (61.3)	Optima MR450w (0.5) Signa (10.6) Signa Excite (41.7) Signa Excite HDx (7.5) Signa Genesis (13.1) Signa HDx (1.0) Signa HDxt (8.5) Signa Twin Speed Excite HD (16.1)	52.6 ± 25.6 18–90	Female (46.7) Male (53.3)
	3T (47.1)	0.2 (7.9) 1.0 (15.2) 1.1 (41.2) 1.2 (35.2) 1.3 (0.6) Unknown (6.9)	Axial (65.0) Sagittal (35.0)	Discovery MR750 (29.9) Signa (5.1) Signa Echospeed (38.4) Signa HDx (2.3) Signa HDxt (24.3)	47.3 ± 22.0 18–89	Female (55.9) Male (44.1)
Philips	**1.5T** (65.1)	1.0 (31.1) 1.1 (68.9)	Axial (61.1) Sagittal (38.9)	ACS III (28.9) Achieva (2.7) Gyroscan Intera (62.1) Gyroscan NT (2.2) Intera (3.7) Intera Achieva (0.4)	45.0 ± 19.1 18–86	Female (50.2) Male (49.8)
	3T (34.9)	1.0 (12.4) 1.1 (69.8) 1.2 (17.5) 1.3 (0.4)	Axial (64.4) Coronal (5.4) Sagittal (30.2)	Achieva (20.7) Gemini (1.1) Ingenia (1.1) Intera (77.1)	46.2 ± 19.1 18–86	Female (42.9) Male (57.1)
Siemens	**1.5T** (33.4)	0.5 (0.4) 1.0 (7.2) 1.2 (13.7) 1.3 (57.9) 1.9 (18.9) 2.0 (1.9) 2.2 (0.2)	Sagittal (100)	Avanto (17.5) Espree (1.2) Sonata (10.2) Sonata Vision (0.2) Symphony (10.2) Trio (2.7) Vision (58.0) Unknown (0.1)	51.7 ± 24.4 18–94	Female (56.4) Male (43.7)
	3T (66.6)	0.3 (2.7) 0.9 (0.1) 1.0 (66.6) 1.1 (0.7) 1.2 (23.4) 1.3 (3.1) 2.3 (3.4)	Axial (0.1) Sagittal (99.9)	Allegra (8.2) Skyra (1.3) Trio (1.9) Trio Tim (81.8) Verio (6.8)	46.2 ± 20.9 18–88	Female (47.8) Male (52.2)

poisoning. Moreover, for PPMI, additional exclusions were made for participants with a Geriatric Depression Scale (Sheikh and Yesavage, 1986) score of more than 5 (inclusion criterion used in the ADNI and AIBL databases).

All original images were visually inspected and four participants were discarded because of evident abnormalities. Five participants with extreme eTIV values were also excluded (Z scores higher than 3.29, $p < .001$). In order to have similar age means between manufacturer and MFS strata, 30 participants of 65 years or older were randomly selected and removed from the GE 1.5T strata. The final sample included 2713 individuals aged between 18 and 94 years (mean: 47.6, SD: 21.7), with a similar proportion of men (n=1361) and women (n=1352). More than half of the scans were acquired using Siemens (n=1550), a third using Philips (n=787), and 14% using GE (n=376) units. Fifty-five percent of the images were obtained using 3T MFS (n=1482). Most of the datasets also had information regarding handedness (78%), race (63%), and education (58%). Based on the available data, the vast majority of the normative sample was right-handed (92%), Caucasian (82%; African 10%; Asian 7%), and had completed high school (95%). Table 2 displays information about age and sex of the participants according to scanner manufacturer and MFS, as well as voxel size and acquisition plane of the scan and the list of scanner models.

Validation samples

We randomly selected 5% of the normative sample (n=137) stratified by manufacturer and MFS to validate the models predicting normative values in an independent sample (Age: 46.6 ± 22.2, range 18–90; 52% female). This validation sample was not used to build the models predicting normative values.

We also validated the normative values using clinical samples of individuals with SZ (n=72; Age: 38.2 ± 13.9, range 18–65; 19% female) from the COBRE dataset and mild AD (n=50 Age: 72.7 ± 7.7, range 56–87; 44% female) randomly selected from the ADNI-2 dataset. SZ was diagnosed using the Structured Clinical Interview for DSM-IV disorders (First et al., 1996). AD was diagnosed according to National Institute of Neurological and Communicative Disorders and Stroke and the Alzheimer's Disease and Related Disorders Association (NINCDS/ADRDA) criteria for probable AD (McKhann et al., 1984) and had a Clinical Dementia Rating of 0.5 or 1.

Segmentation

Cortical segmentation was conducted using *FreeSurfer* (version 5.3), a widely used and freely available automated processing pipeline that quantifies brain anatomy (http://freesurfer.net). All raw T1-weighted images were processed using the "recon-all -all" pipeline with the default set of parameters (no flag options were used). We used the regional cortical surface areas (white surface area), thicknesses, and volumes comprised in the aparc.stats output files, which is the parcellation produced by the default atlas (Desikan-Killiany or DK; Desikan et al., 2006). *Freesurfer* was running on an Ubuntu Server 12.04 LTS platform on a Dell PowerEdge R910 computer with four Intel Xeon E7-4870 2.4 GHz.

The technical details of *FreeSurfer*'s procedures are described in prior publications. Briefly, this processing includes motion correction (Reuter et al., 2010), removal of non-brain tissue using a hybrid watershed/surface deformation procedure (Segonne et al., 2004), automated Talairach transformation, intensity normalization (Sled et al., 1998), tessellation of the gray matter white matter boundary, automated topology correction (Fischl et al., 2001; Segonne et al., 2007), and surface deformation following intensity gradients to optimally place the gray/white and gray/cerebrospinal fluid borders at the location where the greatest shift in intensity defines the transition to the other tissue class (Dale et al., 1999; Dale and Sereno, 1993; Fischl and Dale, 2000). Once the cortical models are complete, a number of deformable procedures can be performed for further data processing and analysis including surface inflation (Fischl et al., 1999a), registration to a spherical atlas which is based on individual cortical folding patterns to match cortical geometry across subjects (Fischl et al., 1999b) and parcellation of the cerebral cortex into units with respect to gyral and sulcal structure (Desikan et al., 2006; Fischl et al., 2004). This method uses both intensity and continuity information from the entire three dimensional MR volume in segmentation and deformation procedures to produce representations of cortical thickness, calculated as the closest distance from the gray/white boundary to the gray/CSF boundary at each vertex on the tessellated surface (Fischl and Dale, 2000). The maps are created using spatial intensity gradients across tissue classes and are therefore not simply reliant on absolute signal intensity. Procedures for the measurement of cortical thickness have been validated against histological analysis (Rosas et al., 2002) and manual measurements (Kuperberg et al., 2003; Salat et al., 2004).

In addition, *FreeSurfer* uses a model-driven approach, matching the new image to a template of manually segmented training set images. Each voxel is then labeled based on the probabilistic information given by the image matching procedure. All structures defined in the *a priori* segmentation are therefore represented in the new image.

Estimated intracranial volume (eTIV; Buckner et al., 2004) was taken from the aseg.stats *Freesurfer* output file. To assure the validity of outermost eTIV values, we verified the registration of the 5% lowest and highest values. Visual inspection of each brain segmentation was conducted using *FreeView* (http://freesurfer.net) by scrolling the entire brain at least through the coronal and axial planes. For each cortical region, the criterion for failed segmentation was inadequate inclusion (e.g. dura mater, ventricle) or omission of approximately 100 voxels or more. The mean percentage of exclusion across regions was 1.8% (SD: 2.5). For analyses on the whole left and right cortical hemispheres, participants with a segmentation error on any of the regions were excluded, resulting in 2073 and 2068 participants, respectively.

We verified the generalizability of the surface areas, thicknesses, and volumes produced by *FreeSurfer* by quantifying the influence of a different hardware setup on these measures (Xubuntu 12.04 on VirtualBox 4.3.10 installed on an iMac 10GB 1067 MHz DDR3 with 2.8 GHz Intel Core i7 and OS X Yosemite 10.10.4). These measures were compared with those generated by the setup used to produce normative values on a random subset of the normative sample (n=50).

Statistical analyses

Surface area, thickness, and volume prediction

Statistical analyses are based on our previously published study on normative data for subcortical regions (Potvin et al., 2016b). Linear regression models predicting cortical measures were built using age, sex, eTIV, MFS, and scanner manufacturer as predictors. Quadratic and cubic terms for age and eTIV were tested, as well as the following interactions: age X sex, eTIV X MFS, MFS X manufacturer, and eTIV X manufacturer. To avoid overfitting and maximize generalizability of the predictions, the best predictive model was determined with a 10-fold cross-validation (Hastie et al., 2008) backward elimination procedure, retaining the model with the subset of predictors that produced the lowest predicted residual sum of squares using SAS 9.4 PROC GLMSELECT (SAS Institute Inc., Cary, NC, USA). For each selected final model, the fit of the data was assessed using R^2 (one minus the regression sum of squares divided by the total sum) and individual predictors' weight was measured by semi-partial eta squares (squared semi-partial correlations). In order to exclude potential abnormalities and produce valid predictive model for each brain subdivision, outliers with surface area/thickness/volume Z scores higher than 3.29 ($p < .001$) were excluded. Depending on the region, between 0 and 33 outliers out of 2713 were excluded.

Validation

In addition to the cross-validation procedure, the predictions of the models were validated using the independent validation sample of healthy controls by first calculating a validation R^2 (squared correlation between observed and predicted measures). Then, we tested the mean difference between observed and predicted cortical measures using independent two-sample *t*-tests (since predicted values are not produced using the observed measure and thus, observed and predicted measures are not correlated) with Bonferroni correction.

We then examined the validity of the normative values to show expected patterns of normality deviations using the Z score effect sizes (described below) in the validation samples of healthy individuals and of individuals with AD and SZ.

Finally, with the available data (see Table 2), we assessed the influence of voxel size and plane acquisition on cortical surface, thickness and volume by adding these variables to the final models. We also assessed the impact of a different computer hardware setup on the cortical measures generated by *FreeSurfer* using dependent one-sample *t*-tests with Bonferroni correction.

Normative statistics

Z score effect sizes (Z_{OP}) were obtained by subtracting the *Observed value* from the *Predicted value* divided by the root mean square error (also called residual standard deviation or standard error of estimate) of the model predicting normative values (Crawford et al., 2012). In order to automatically calculate normative Z scores for multiple individuals, we also provide a python script as Supplementary material. Furthermore, based on work from Crawford and colleagues (Crawford and Garthwaite, 2006; Crawford et al., 2012), we also provide as Supplementary material a Microsoft Excel spreadsheet producing various normative statistics for an individual, including prediction intervals, single case significance test of value abnormality, effect size and estimated percentage of the normative population with a smaller surface area, thickness or volume. Single case significance test of value abnormality was computed by the formula below, a *t*-statistic with N - k (number of predictors) −1 degrees of freedom using the difference between actual (Y_0) and predicted ($\hat{Y}$) values, divided by the standard error of the predicted value where $S_{Y \cdot X}$ represents the root mean square error of the model predicting normative values, r^{ii} identifies off-diagonal elements of the inverted correlation matrix for the k predictor variables, r^{ij} identifies elements in the main diagonal, and $z_0 = (z_{i0}, \ldots, z_{k0})$ identifies the patient's scores on the predictor variables in Z score

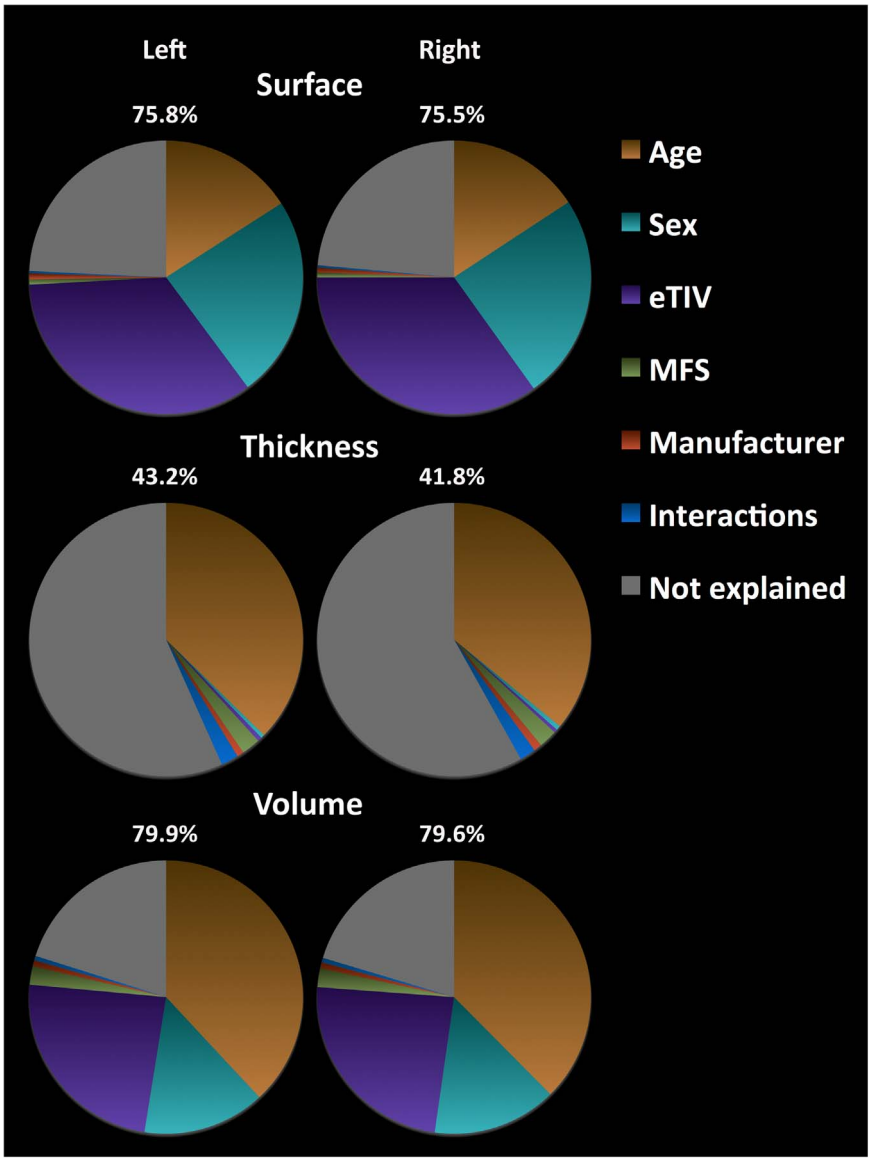

Fig. 1. Explained variance (R^2) for left and right cortical hemispheres according to each predictor.

form (Crawford and Garthwaite, 2006).

$$\frac{Y_0 - \hat{\mathbf{Y}}}{S_{Y\bullet X}\sqrt{1+\frac{1}{N}+\frac{1}{N-1}\sum r^{ii}z_{io}^2+\frac{2}{N-1}\sum r^{ij}z_{io}z_{jo}}}$$

This procedure also yields an unbiased point estimate of the value abnormality that can be supplemented with confidence intervals following a non-central *t*-distribution (Crawford and Garthwaite, 2006).

Results

Prediction of cortical surface areas, thicknesses, and volumes

Cortical hemispheres

Fig. 1 displays the explained variance (R^2) for the whole left and right cortical hemispheres. The models for surface area and volume explained a high amount of variance, nearly twice the variance of that of the thickness models. Age, sex and eTIV predicted most of the variance for surface area and volume while age was the main predictor for thickness. Fig. 2 illustrates the effects related to the participants' characteristics using standardized predicted values. For all figures, fits were standardized according to the standard deviation of the true values. Age and eTIV had similar effects for surface area and volume, which were relatively linear. Surface area and volume decreased by approximately one and two standard deviations (SD) from 18 to 96 years, respectively. In opposition, the reduction of cortical thickness according to age was non-linear as it became more pronounced after the 6th decade of life and dropped by more than three SDs across adulthood. In contrast to surface area and volume results, eTIV had little effect on cortical thickness. Men had clearly larger bilateral surface area and volume than women (approximately 1SD), but thickness was similar.

Fig. 3 shows the standardized fitted values for the effects related to the scanner. The strongest effects were for cortical thickness, followed by volume. For GE and Siemens manufacturer, there was a difference of at least half a SD between 3T and 1.5T MFS in terms of mean predicted values, with 1.5T resulting in a reduced volume and thickness.

Cortical regions

Coefficients predicting cortical surface areas, thicknesses, and volumes are shown in Tables 3–5, respectively. The mean explained variance for all regions was 41% (range: 16–64) for surface areas, 27%

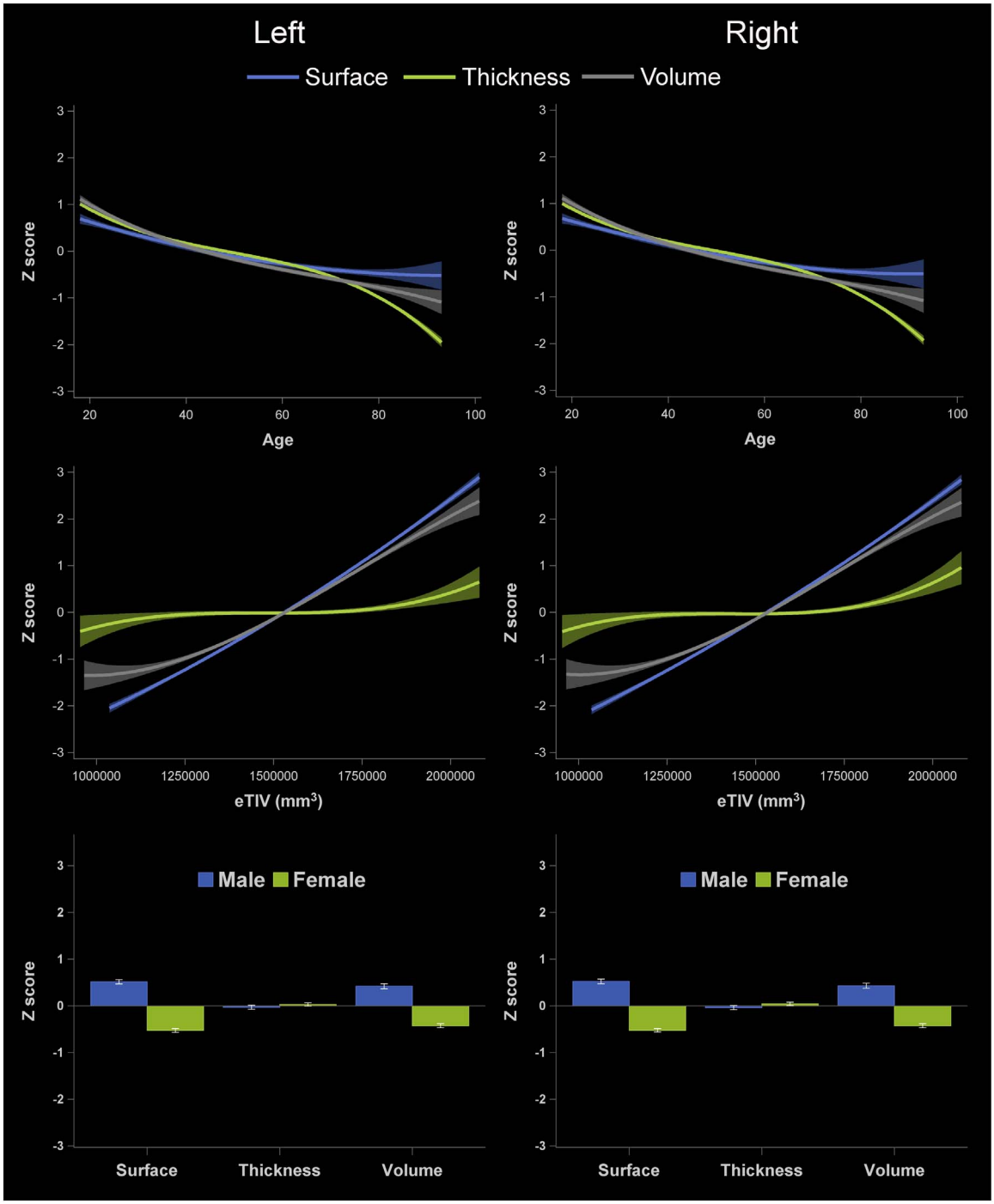

Fig. 2. Illustration of participants' characteristics effects on morphometry of the cortical hemispheres. Y axis represent standardized values according to the standard deviation. Top row: age effects. Middle row: eTIV effects. Bottom row: Sex effects. Error bars and shaded ribbons denote 95% confidence intervals.

(range 10–45) for thicknesses, and 46% (range 13–72) for volumes. Fig. 4 illustrates the R^2 related to each predictor according to each cortical region measure. In general, age was the best predictor for most regional thicknesses and volumes while eTIV was the best predictor for most regional surface areas. Figs. 5 to 8 illustrate the age effects on cortical surface areas, thicknesses, and volumes for each region. The effect of age was heterogeneous across regions. For example, unlike most regions, many temporal regions showed that thickness slightly increased between the second and fifth decade of age before decreasing. Indeed, for thickness in these temporal regions (e.g. entorhinal and temporal pole), age had little R^2 (< 2%), indicating minor predictive value compared to other regions (overall mean: 21%).

Together, scanner characteristics (manufacturer, MFS, and their interaction) generally predicted a limited amount of variance, but their effects were stronger for thickness (mean: 7%, range: 1–25%) than surface area (mean: 1%, range: 0–4%) and volume (mean: 3%, range: 0–10%).

Validation

Healthy controls

For the whole cortical hemispheres, the generalization of the models was satisfactory as shown by the mean difference between validation and original R^2 (Left/Right): 1.0%/–1.6% for surface area,

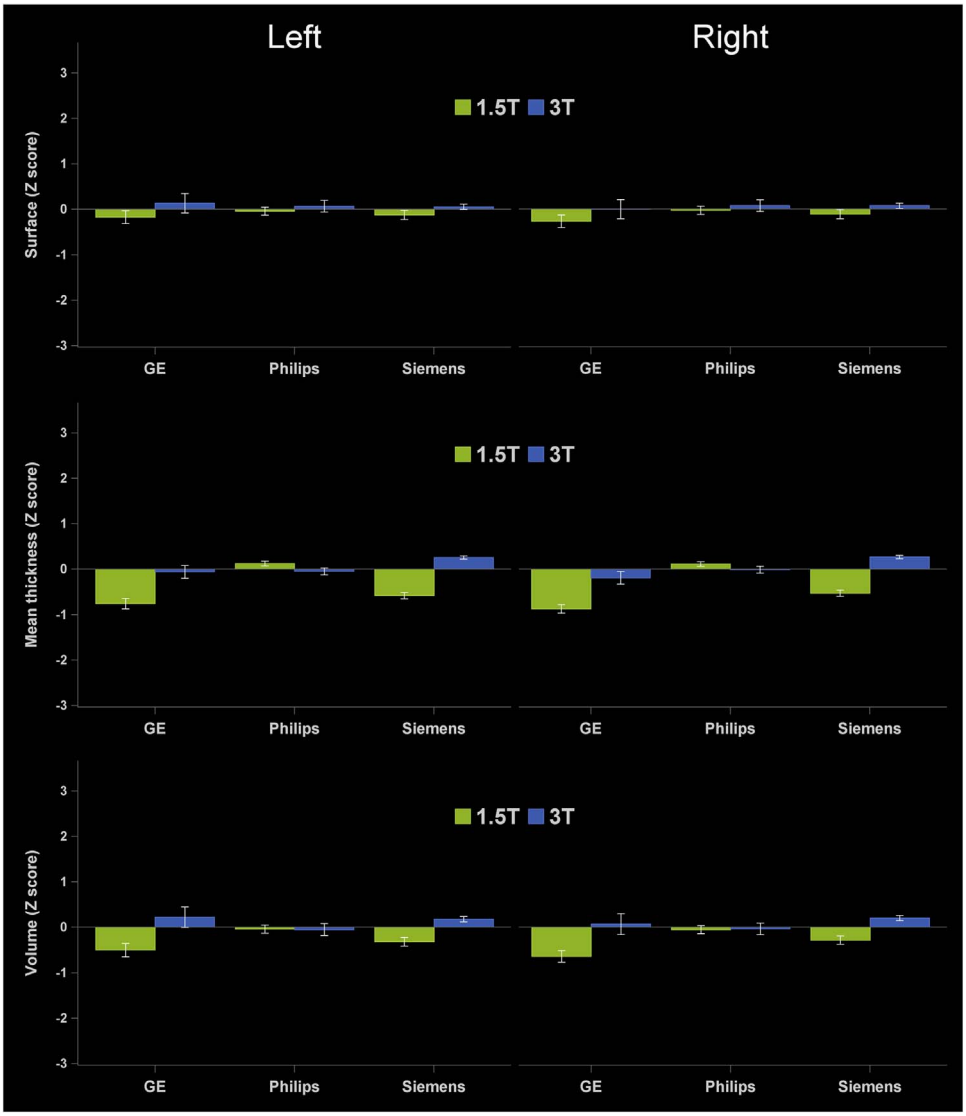

Fig. 3. Illustration of scanner manufacturer and magnetic field strength effects on morphometry of the cortical hemispheres. Y axis represent standardized values according to the standard deviation. Top row: Surface area. Middle row: Thickness. Bottom row: Volume. Error bars and shaded ribbons denote 95% confidence intervals.

12.5%/10.4% for thickness, and 2.5%/2.4% for volume (positive values meaning that the prediction in the independent sample was better than in the sample used to build the model).

For regional cortical volumes, the mean difference between validation and original R^2 was 1.6% (range −12 to 11%) for surface areas, 4.8% (range −5 to 18%) for thicknesses, and 1.5% (range −10 to 11%) for volumes, which shows adequate generalization of the models (Supplemental Fig. 1). The largest negative discrepancies were for bilateral caudal middle frontal surface areas (−12%), the right caudal middle frontal volume (−10%) and the right supramarginal volumes (−9%).

None of the mean actual surface areas, thicknesses, and volumes significantly differed from the mean predicted normative values (Supplemental Table 1) and the mean Z_{OP} effect size indicated very little deviation from the normative values across regions (mean surface areas: −0.04, SD: 0.08, range −0.25 to 0.18; mean thicknesses: 0.03, SD: 0.07, range −0.10 to 0.20; mean volumes: −0.03, SD: 0.09, range −0.24 to 0.19).

Schizophrenia and Alzheimer's disease

Fig. 9 shows the Z_{OP} effect size for the SZ and AD groups for each mean regional cortical surface area, thickness, and volume. In the SZ group, several cortical measures were substantially lower than the expected normative values. The strongest effect sizes included both cortical hemispheres volumes and bilateral lateral orbitofrontal, superior temporal, lingual, and fusiform volumes. The mean Z_{OP} effect size for SZ indicated small to moderate deviations from the normative values across regions (mean surface areas: −0.44, SD: 0.21, range −0.95 to −0.02; mean thicknesses: −0.55, SD: 0.24, range −0.94 to 0.22; mean volumes: −0.76, SD: 0.30, range −1.66 to −0.17).

In the mild AD group, multiple regional cortical measures were also substantially lower than the expected normative values. The strongest effect sizes included bilateral entorhinal and inferior temporal thicknesses and volumes, fusiform thickness, and inferior parietal thicknesses. The mean Z_{OP} effect size for AD indicated small to moderate deviations from the normative values across regions (mean surface areas: −0.33, SD: 0.26, range −1.02 to 0.20; mean thicknesses: −0.55, SD: 0.45, range −1.61 to 0.39; mean volumes: −0.41, SD: 0.39, range −1.33 to 0.28). Fig. 10 shows examples of the distribution of effect sizes among the validation samples for the results discussed above.

Influence of voxel size and acquisition plane

Further analyses showed that voxel size and acquisition plane had

Table 3
Coefficients of models predicting left (L) and right (R) regional cortical surface area.

			Sociodemographics				Estimated total intracranial volume (eTIV)			Scanner			Interactions					
Region	**RMSE**	**Int**	**Age**	**Age^2**	**Age^3**	**Sex**	**eTIV**	**eTIV^2**	**eTIV^3**	**Strength**	**Manufacturer**		**GE X MFS**	**Philips X MFS**	**eTIV X MFS**	**Age X Sex**	**eTIV X GE**	**eTIV X Philips**
						M / F				**1.5 T / 3 T**	**GE /Siemens**	**Philips /Siemens**						
Superior temporal L	327.29	3683.3	**−3.79E+00**	−3.14E-02	–	**8.40E+01**	**1.73E-03**	**4.84E-10**	–	*4.91E+01*	5.01E+00	−3.45E+01	−8.10E+01	**−1.20E+02**	*1.97E-04*	*−1.36E+00*	−1.51E-04	−1.71E-04
Superior temporal R	285.48	3535.6	**−4.58E+00**	–	–	–	**1.64E-03**	6.21E-10	–	*3.75E+01*	−2.91E+01	**−5.42E+01**	−5.84E+01	**−8.71E+01**	*1.46E-04*	–	−1.06E-04	**−2.25E-04**
Middle temporal L	311.30	3050.8	**−4.52E+00**	**−8.89E-02**	–	**4.25E+01**	**1.71E-03**	*3.33E-10*	*−1.19E-15*	**−5.79E+01**	−5.33E+00	**−1.13E+02**	4.45E+00	**1.02E+02**	–	−9.70E-01	1.61E-05	**−2.99E-04**
Middle temporal R	324.22	3361.8	**−4.22E+00**	−3.75E-02	−1.62E-03	*3.38E+01*	**1.92E-03**	*3.54E-10*	**−1.54E-15**	**−5.76E+01**	7.05E+00	**−7.96E+01**	−4.79E+01	4.07E+01	–	−1.06E+00	1.85E-04	*−1.77E-04*
Inferior temporal L	370.55	3228.8	**−5.11E+00**	**−8.36E-02**	–	**5.16E+01**	**1.84E-03**	**6.35E-10**	*−1.35E-15*	7.01E+00	**1.51E+02**	−2.83E+01	**−1.78E+02**	−7.19E+00	–	−7.61E-01	1.61E-04	*−1.91E-04*
Inferior temporal R	346.76	3147.4	**−4.83E+00**	**−8.23E-02**	–	*4.33E+01*	**1.75E-03**	**4.41E-10**	–	**−8.35E+01**	2.33E+01	**−7.73E+01**	−5.14E+01	*8.78E+01*	–	–	−3.26E-05	**−2.47E-04**
Transverse temporal L	69.73	457.3	**−3.85E-01**	−7.65E-03	–	*7.88E+00*	**2.09E-04**	*7.12E-11*	−1.40E-16	3.10E+00	−2.51E+00	3.73E+00	−1.47E+01	−3.00E+01	–	–	–	–
Transverse temporal R	50.99	340.0	**−2.99E-01**	**−1.17E-02**	–	*5.21E+00*	**1.46E-04**	4.53E-11	–	2.84E+00	2.87E+00	6.05E+00	−8.15E+00	−2.44E+01	–	–	–	–
Temporal pole L	54.47	462.0	**−4.76E-01**	–	–	**1.38E+01**	**1.45E-04**	−4.69E-12	−8.07E-17	**1.76E+01**	2.51E+00	−1.89E+00	*−1.42E+01*	**−2.06E+01**	–	–	*4.16E-05*	−1.56E-05
Temporal pole R	56.60	420.0	**−1.99E-01**	–	–	**8.84E+00**	**1.19E-04**	–	–	–	1.59E+00	**−1.29E+01**	–	–	–	–	–	–
Banks sts L	146.10	1028.7	**−9.74E-01**	−6.43E-03	−6.80E-04	**2.78E+01**	**4.83E-04**	**1.99E-10**	–	**−2.38E+01**	−1.51E+01	**−2.72E+01**	–	–	–	–	−1.25E-05	−4.23E-05
Banks sts R	120.47	941.5	**−1.27E+00**	−1.34E-02	–	**1.73E+01**	**4.30E-04**	*1.07E-10*	−3.03E-16	**−1.55E+01**	**−3.34E+01**	**−2.42E+01**	–	–	–	–	6.80E-05	−4.87E-05
Entorhinal L	67.47	389.9	*3.83E-01*	**−1.87E-02**	**−6.70E-04**	**1.94E+01**	**1.85E-04**	*6.92E-11*	–	4.52E+00	*9.71E+00*	**1.27E+01**	–	–	–	–	–	–
Entorhinal R	70.09	355.0	9.71E-02	**−1.68E-02**	–	**1.16E+01**	**1.84E-04**	**1.00E-10**	–	**−2.22E+01**	**−2.19E+01**	**−2.44E+01**	**4.26E+01**	**3.11E+01**	3.10E-05	–	−3.86E-05	**−6.28E-05**
Fusiform L	339.88	3231.8	**−3.29E+00**	−2.21E-02	*−2.74E-03*	*4.39E+01*	**1.65E-03**	2.64E-10	**−2.01E-15**	*−3.31E+01*	−3.17E+01	**−6.74E+01**	–	–	–	−8.88E-01	–	–
Fusiform R	323.90	3152.4	**−3.12E+00**	*−5.51E-02*	−1.55E-03	**1.07E+02**	**1.54E-03**	**4.39E-10**	−8.63E-16	**−1.06E+02**	−7.48E+00	**−9.98E+01**	−3.12E+01	5.11E+01	–	−9.38E-01	1.21E-04	*−1.85E-04*
Parahippocampal L	85.66	707.2	**−1.24E+00**	**−2.58E-02**	–	–	**3.20E-04**	**1.78E-10**	−2.25E-16	**−1.03E+01**	−2.50E+00	**−1.89E+01**	–	–	–	–	–	–
Parahippocampal R	80.94	677.0	**−1.06E+00**	**−1.94E-02**	–	**1.30E+01**	**2.97E-04**	**1.22E-10**	–	**−2.25E+01**	1.57E+00	**−1.53E+01**	–	–	–	–	**7.34E-05**	−2.52E-05
Superior frontal L	576.23	7110.2	**−1.19E+01**	*−7.06E-02*	–	**1.18E+02**	**3.59E-03**	**1.10E-09**	–	5.89E+01	−2.80E+01	**−2.03E+02**	**−2.84E+02**	−1.04E+02	–	–	*4.13E-04*	−2.19E-04
Superior frontal R	587.65	6901.2	**−1.07E+01**	*−7.57E-02*	–	**1.10E+02**	**3.68E-03**	**1.03E-09**	*−2.19E-15*	*7.55E+01*	*−1.07E+02*	**−1.70E+02**	**−2.10E+02**	**−1.49E+02**	–	−1.34E+00	–	–
Rostral middle frontal L	554.40	5595.1	**−1.13E+01**	–	–	**1.05E+02**	**3.06E-03**	**7.10E-10**	–	*−5.46E+01*	*−7.02E+01*	**−1.70E+02**	–	–	–	–	–	–
Rostral middle frontal R	581.91	5723.6	**−1.16E+01**	–	–	**1.27E+02**	**3.14E-03**	**1.25E-09**	–	*−5.11E+01*	*−8.74E+01*	**−1.06E+02**	–	–	–	–	3.33E-04	−2.42E-04
Caudal middle frontal L	320.95	2295.9	**−4.24E+00**	–	–	–	**1.45E-03**	**3.89E-10**	*−1.21E-15*	−1.01E+01	−8.14E+00	**−7.22E+01**	−6.85E+01	1.23E+01	–	–	1.57E-04	−1.26E-04

(continued on next page)

Table 3 *(continued)*

Region	RMSE	Int	Sociodemographics				Estimated total intracranial volume (eTIV)			Scanner			Interactions					
			Age	Age^2	Age^3	Sex	eTIV	eTIV^2	eTIV^3	Strength	Manufacturer		GE X MFS	Philips X MFS	eTIV X MFS	Age X Sex	eTIV X GE	eTIV X Philips
						M / F				1.5 T / 3 T	GE /Siemens	Philips /Siemens						
Caudal middle frontal R	313.89	2107.4	**−4.25E+00**	–	–	–	**1.48E-03**	*3.44E-10*	**−1.53E-15**	3.40E+01	2.87E+01	−3.10E+01	**−1.06E+02**	−6.04E+01	–	–	1.59E-04	*−1.77E-04*
Pars opercularis L	226.18	1630.7	**−2.58E+00**	–	–	1.92E+01	**7.64E-04**	1.94E-10	–	−1.24E+01	2.98E+00	**−4.32E+01**	**−9.13E+01**	−1.08E+01	6.51E-05	*−8.47E-01*	3.36E-05	*−1.13E-04*
Pars opercularis R	194.81	1391.9	**−2.28E+00**	*−2.41E-02*	–	–	**7.44E-04**	1.22E-10	**−9.02E-16**	1.56E+01	−2.29E+01	**−4.20E+01**	*−5.96E+01*	−1.55E+01	–	–	–	–
Pars triangularis L	170.02	1259.1	**−2.34E+00**	–	–	**4.80E+01**	**4.73E-04**	**2.21E-10**	–	**−1.94E+01**	**−3.25E+01**	**−5.01E+01**	–	–	–	–	–	–
Pars triangularis R	207.57	1445.5	**−2.72E+00**	–	–	**6.04E+01**	**5.12E-04**	1.87E-10	–	−1.02E+01	**−4.83E+01**	**−5.29E+01**	–	–	*1.03E-04*	*−7.74E-01*	–	–
Pars orbitalis L	70.38	626.1	**−5.79E-01**	−1.27E-02	−3.44E-04	**1.06E+01**	**3.15E-04**	*7.77E-11*	*−2.18E-16*	**−1.25E+01**	*−9.96E+00*	**−1.19E+01**	–	–	*−3.68E-05*	–	–	–
Pars orbitalis R	85.17	754.5	**−9.97E-01**	*−1.01E-02*	–	**2.98E+01**	**3.01E-04**	7.19E-11	–	*−8.58E+00*	**−1.38E+01**	**−1.58E+01**	–	–	–	−3.07E-01	4.68E-05	−1.53E-05
Lateral orbitofrontal L	245.72	2624.1	**−1.79E+00**	−2.23E-02	*−1.62E-03*	1.89E+01	**1.33E-03**	2.21E-10	**−1.05E-15**	**−1.27E+02**	**−1.25E+02**	**−8.81E+01**	4.00E+01	**9.49E+01**	–	–	*1.83E-04*	−1.02E-04
Lateral orbitofrontal R	263.19	2531.2	**−3.25E+00**	**−5.13E-02**	–	–	**1.33E-03**	*2.75E-10*	**−1.13E-15**	**4.02E+01**	1.68E+01	1.14E+01	**−1.09E+02**	*−5.48E+01*	*−1.34E-04*	–	**2.52E-04**	−6.42E-06
Medial orbitofrontal L	196.81	1850.3	**−1.06E+00**	**−4.13E-02**	–	–	**1.13E-03**	*2.21E-10*	**−1.10E-15**	2.34E+01	**5.55E+01**	**−6.03E+01**	**−8.95E+01**	−2.18E+00	–	–	3.71E-05	**−1.57E-04**
Medial orbitofrontal R	165.04	1833.0	**−1.10E+00**	−1.24E-02	−7.54E-04	**3.12E+01**	**8.29E-04**	3.41E-11	−3.83E-16	**−3.24E+01**	**−3.15E+01**	**−7.00E+01**	–	–	–	–	2.96E-05	*−1.00E-04*
Precentral L	409.33	4760.9	**−4.79E+00**	–	–	**1.50E+02**	**1.90E-03**	**7.64E-10**	–	**6.29E+01**	**−1.03E+02**	**−1.86E+02**	–	–	*2.14E-04*	–	2.69E-04	−1.34E-04
Precentral R	411.39	4791.0	**−3.53E+00**	–	–	**1.47E+02**	**1.95E-03**	**6.47E-10**	*1.65E-15*	**9.34E+01**	**−1.01E+02**	**−1.42E+02**	*−9.98E+01*	−5.34E+01	*2.46E-04*	−1.05E+00	8.26E-05	−2.02E-04
Paracentral L	159.94	1345.6	**−1.00E+00**	–	–	−1.25E+00	**6.52E-04**	**2.90E-10**	*−5.76E-16*	*1.45E+01*	**−6.50E+01**	**−5.54E+01**	–	–	–	−4.97E-01	–	–
Paracentral R	188.98	1527.5	**−1.41E+00**	−1.61E-02	–	–	**7.22E-04**	**2.83E-10**	–	**4.36E+01**	**−4.37E+01**	−1.15E+01	−3.80E+01	**−6.76E+01**	–	–	–	–
Frontal pole L	32.67	198.6	**−2.28E-01**	**6.63E-03**	−1.51E-04	**4.29E+00**	**6.46E-05**	*3.28E-11*	–	2.84E+00	1.33E+00	−1.57E+00	*−8.06E+00*	**−1.33E+01**	–	–	–	–
Frontal pole R	41.68	265.1	**−3.85E-01**	**7.51E-03**	–	**1.09E+01**	**7.26E-05**	*4.66E-11*	7.34E-17	**1.00E+01**	**9.43E+00**	2.25E+00	**−1.70E+01**	**−2.29E+01**	–	−1.26E-01	–	–
Postcentral L	365.42	4113.0	**−3.12E+00**	*5.16E-02*	−1.48E-03	**7.93E+01**	**1.94E-03**	3.37E-10	*−1.24E-15*	–	**−1.09E+02**	**−1.23E+02**	–	–	–	–	–	–
Postcentral R	362.44	3945.5	**−3.91E+00**	*4.79E-02*	–	**6.48E+01**	**1.83E-03**	*3.87E-10*	−9.78E-16	–	**−9.09E+01**	**−1.18E+02**	–	–	–	–	–	–
Supramarginal L	425.68	3781.8	**−4.44E+00**	–	–	**1.07E+02**	**2.21E-03**	**5.54E-10**	**−2.44E-15**	−1.46E+01	1.19E+01	−3.69E+01	*−1.26E+02*	−6.71E+01	–	–	–	–
Supramarginal R	412.22	3642.2	**−4.01E+00**	–	–	*4.92E+01*	**1.91E-03**	**8.31E-10**	**−1.84E-15**	–	**−9.96E+01**	**−1.13E+02**	–	–	–	*−1.72E+00*	–	–
Superior parietal L	517.87	5371.7	**−7.63E+00**	−5.38E-02	–	–	**2.48E-03**	**7.51E-10**	**−2.16E-15**	4.51E+01	−2.28E+01	−6.41E+01	*−1.32E+02*	−9.80E+01	–	–	3.39E-04	2.06E-04
Superior parietal R	503.72	5394.8	**−6.48E+00**	−5.28E-02	–	4.26E+01	**2.36E-03**	4.47E-10	–	–	**−1.29E+02**	**−1.57E+02**	–	–	–	−1.52E+00	–	–

(continued on next page)

Table 3 *(continued)*

Region	RMSE	Int	Sociodemographics				Estimated total intracranial volume (eTIV)			Scanner			Interactions					
			Age	Age^2	Age^3	Sex	eTIV	eTIV^2	eTIV^3	Strength	Manufacturer		GE X MFS	Philips X MFS	eTIV X MFS	Age X Sex	eTIV X GE	eTIV X Philips
						M / F				1.5 T / 3 T	GE /Siemens	Philips /Siemens						
Inferior parietal L	497.82	4497.4	**−3.67E+00**	5.65E-02	*−3.77E-03*	**8.57E+01**	**2.21E-03**	4.04E-10	−9.21E-16	−8.64E+00	*−6.88E+01*	**−1.11E+02**	–	–	*2.68E-04*	**−2.51E+00**	2.05E-04	−1.70E-04
Inferior parietal R	564.52	5319.0	**−5.48E+00**	2.93E-02	*−3.94E-03*	**2.22E+02**	**2.45E-03**	*5.73E-10*	–	**−1.23E+02**	**−1.45E+02**	**−2.42E+02**	−2.28E+01	*1.16E+02*	2.28E-04	–	2.61E-04	−2.21E-04
Precuneus L	354.05	3738.9	**−4.84E+00**	–	–	**6.40E+01**	**1.95E-03**	2.97E-10	**−1.67E-15**	−1.56E+01	**−1.52E+02**	−4.73E+01	−2.11E+01	*−8.09E+01*	–	−1.08E+00	–	–
Precuneus R	384.47	3887.9	**−5.89E+00**	1.97E-02	–	**8.82E+01**	**2.01E-03**	**6.30E-10**	*−1.26E-15*	*−3.77E+01*	**−1.57E+02**	**−9.12E+01**	–	–	–	–	–	–
Lingual L	362.89	3062.4	−6.94E-01	*−5.33E-02*	*−2.66E-03*	**6.90E+01**	**1.25E-03**	2.06E-10	−8.48E-16	**−1.40E+02**	**−1.32E+02**	**−8.49E+01**	**1.59E+02**	3.54E+01	–	−1.14E+00	−2.29E-05	**−2.36E-04**
Lingual R	347.33	3100.8	**−3.08E+00**	**−7.81E-02**	–	**5.24E+01**	**1.10E-03**	2.53E-10	–	**−1.21E+02**	**−1.09E+02**	**−9.56E+01**	*1.02E+02*	*7.52E+01*	–	–	4.01E-05	*−2.04E-04*
Pericalcarine L	214.72	1376.5	**−1.56E+00**	–	–	1.93E+01	**5.64E-04**	**3.00E-10**	–	**−8.70E+01**	**−9.79E+01**	**−4.73E+01**	**1.11E+02**	**6.61E+01**	–	–	1.35E-05	**−1.41E-04**
Pericalcarine R	225.87	1527.5	**−1.39E+00**	−2.35E-02	–	1.89E+01	**7.11E-04**	**2.93E-10**	−5.67E-16	**−8.12E+01**	**−8.66E+01**	**−6.15E+01**	**7.70E+01**	**8.41E+01**	**−1.37E-04**	–	–	–
Cuneus L	178.51	1452.2	**−1.49E+00**	**−3.43E-02**	–	**4.27E+01**	**5.03E-04**	–	–	**−2.95E+01**	**−8.62E+01**	−1.64E+01	**9.18E+01**	8.32E+00	–	**−9.13E-01**	–	–
Cuneus R	172.17	1494.9	**−1.78E+00**	*−2.47E-02*	–	**3.87E+01**	**6.82E-04**	1.34E-10	*−5.57E-16*	–	**−3.76E+01**	−2.55E+00	–	–	–	–	–	–
Lateral occipital L	474.63	4678.8	**−6.52E+00**	*−6.69E-02*	–	**1.68E+02**	**2.00E-03**	**7.97E-10**	–	–	*−5.94E+01*	**−7.25E+01**	–	–	–	–	9.03E-05	*−2.55E-04*
Lateral occipital R	475.56	4534.4	**−5.95E+00**	–	–	**1.84E+02**	**2.16E-03**	**6.26E-10**	−1.41E-15	–	**−1.05E+02**	*−5.34E+01*	–	–	–	−1.44E+00	−1.79E-04	*−2.81E-04*
Rostral anterior cingulate L	130.71	851.8	5.65E-02	−1.58E-02	−5.57E-04	2.42E+00	**5.98E-04**	**1.94E-10**	**−6.04E-16**	**−3.88E+01**	**−5.50E+01**	**−2.75E+01**	1.47E+01	*2.69E+01*	–	*5.16E-01*	6.62E-05	−5.47E-05
Rostral anterior cingulate R	119.00	698.4	**−3.45E-01**	*−1.65E-02*	–	7.23E+00	**4.65E-04**	**1.77E-10**	*−4.07E-16*	**−3.13E+01**	**−2.80E+01**	**−2.15E+01**	–	–	–	–	4.79E-05	−3.29E-05
Caudal anterior cingulate L	124.21	648.5	−2.81E-01	3.06E-03	−5.53E-04	−8.26E+00	**3.76E-04**	**1.41E-10**	−2.84E-16	–	**−1.91E+01**	**−2.04E+01**	–	–	–	–	*9.86E-05*	−1.48E-05
Caudal anterior cingulate R	140.39	793.6	−4.64E-01	−1.94E-03	−5.80E-04	−1.63E-01	**4.32E-04**	6.22E-11	*−4.81E-16*	**−1.62E+01**	**−3.97E+01**	**−2.83E+01**	–	–	–	4.24E-01	7.80E-05	−2.41E-05
Posterior cingulate L	149.37	1157.3	**−1.20E+00**	1.14E-02	−5.90E-04	**3.04E+01**	**5.54E-04**	3.39E-11	**−6.61E-16**	*−2.18E+01*	**−8.67E+01**	**−4.50E+01**	*4.44E+01*	−8.90E-01	–	*−5.69E-01*	*1.05E-04*	−3.55E-06
Posterior cingulate R	150.04	1211.0	**−1.72E+00**	*−1.79E-02*	–	–	**7.00E-04**	**1.81E-10**	**−6.70E-16**	**−1.93E+01**	**−8.73E+01**	**−3.79E+01**	–	–	−3.95E-05	–	–	–
Isthmus cingulate L	144.62	1001.6	**−6.07E-01**	–	–	**3.11E+01**	**6.35E-04**	*1.28E-10*	**−8.44E-16**	–	**−6.17E+01**	**−5.87E+01**	–	–	–	–	–	–
Isthmus cingulate R	129.53	933.0	**−6.54E-01**	–	–	**2.15E+01**	**5.38E-04**	**2.48E-10**	–	**2.30E+01**	**−5.12E+01**	**−4.42E+01**	−2.28E+00	−2.22E+01	–	–	–	–
Insula L	179.50	2214.6	−1.88E-01	**−4.36E-02**	–	–	**1.08E-03**	**4.54E-10**	–	*−2.23E+01*	*−3.06E+01*	−1.57E+01	−1.14E+01	*−4.35E+01*	–	–	–	–
Insula R	211.82	2275.0	*4.46E-01*	**−7.20E-02**	–	**3.23E+01**	**1.13E-03**	**3.65E-10**	–	**−4.13E+01**	−3.22E+01	**−6.87E+01**	4.47E+00	**8.44E+01**	–	–	1.16E-04	−3.10E-05
Cortex L	4587.01	83692.6	**−1.03E+02**	−6.18E-01	−2.83E-02	**1.36E+03**	**4.30E-02**	**9.02E-09**	**−2.83E-14**	−3.04E+02	**8.63E+02**	−1.25E+03	*−1.61E+03*	−1.28E+03	–	–	*1.51E-03*	−3.45E-03
Cortex R	4566.49	84184.8	**−1.07E+02**	**−8.32E-01**	**−2.18E-02**	**1.55E+03**	4.09E-02	8.85E-09	–	**−2.46E+02**	**6.27E+02**	−1.22E+03	**−1.95E+03**	−1.29E+03	*1.53E-03*	–	−5.49E-04	−4.54E-03

Note. Categories are coded 0 and 1 with reference categories (Female, Siemens, and 3T) coded 0. Age and eTIV are centered by the mean (Age – 47.58; eTIV – 1528926.15). Int: Intercept. RMSE: Root mean square error. STS: Superior temporal sulcus. *Italic* $p < .05$; **Bold** $p < .01$.

Table 4
Coefficients of models predicting left (L) and right (R) regional cortical thickness.

			Sociodemographics				Estimated total intracranial volume (eTIV)			Scanner			Interactions					
Region	RMSE	Int	Age	Age^2	Age^3	Sex	eTIV	eTIV^2	eTIV^3	Strength	Manufacturer		GE X MFS	Philips X MFS	eTIV X MFS	Age X Sex	eTIV X GE	eTIV X Philips
						M / F				1.5 T / 3 T	GE /Siemens	Philips /Siemens						
Superior temporal L	0.1552	2.7781	**−3.60E-03**	**−3.27E-05**	*−1.18E-06*	**−2.22E-02**	**9.51E-08**	–	–	**−1.35E-01**	**−5.80E-02**	**−3.67E-02**	**9.89E-02**	**1.30E-01**	–	−5.21E-04	–	–
Superior temporal R	0.1605	2.7896	**−3.59E-03**	**−3.07E-05**	−8.85E-07	−1.26E-02	**8.67E-08**	–	–	**−1.50E-01**	**−8.52E-02**	1.16E-02	**1.54E-01**	**1.23E-01**	–	−5.81E-04	–	–
Middle temporal L	0.1721	2.8330	**−2.10E-03**	8.40E-06	**−1.82E-06**	–	**1.09E-07**	–	–	**−1.70E-01**	**−4.35E-02**	−1.10E-02	**1.38E-01**	**1.52E-01**	–	–	−7.02E-08	−8.03E-08
Middle temporal R	0.1696	2.8792	**−2.70E-03**	−2.01E-05	–	−9.09E-03	**9.33E-08**	−1.08E-13	–	**−1.70E-01**	**−6.54E-02**	6.39E-03	**1.63E-01**	**1.62E-01**	–	*−6.62E-04*	5.94E-09	*−8.92E-08*
Inferior temporal L	0.1789	2.7508	**−1.12E-03**	**−4.14E-05**	–	**−2.40E-02**	**1.12E-07**	–	–	**−1.19E-01**	−2.57E-02	−3.84E-03	**1.28E-01**	**1.45E-01**	4.31E-08	–	−1.09E-07	*−1.03E-07*
Inferior temporal R	0.1873	2.7874	*1.03E-03*	−1.87E-05	**−1.68E-06**	−1.09E-02	**1.46E-07**	–	–	**−2.17E-01**	*−4.49E-02*	−2.06E-02	**1.94E-01**	**2.41E-01**	–	*−8.92E-04*	*−1.55E-07*	**−1.53E-07**
Transverse temporal L	0.2239	2.3293	**−3.62E-03**	**5.17E-05**	**−1.89E-06**	**−7.09E-02**	**1.12E-07**	–	–	−1.98E-02	−1.38E-02	**−1.27E-01**	−2.95E-02	1.01E-01	–	–	–	–
Transverse temporal R	0.2333	2.3716	**−3.32E-03**	*4.21E-05*	*−1.68E-06*	**−6.87E-02**	**1.87E-07**	−1.80E-13	–	**−4.55E-02**	3.85E-03	**−1.03E-01**	−3.28E-02	**1.21E-01**	*1.12E-07*	–	−1.29E-07	*−1.34E-07*
Temporal pole L	0.3387	3.6002	**1.44E-03**	**−6.31E-05**	–	2.44E-02	*−1.46E-07*	−1.94E-13	8.30E-19	**−2.44E-01**	−2.85E-02	**1.76E-01**	**2.28E-01**	**2.11E-01**	–	*−1.66E-03*	–	–
Temporal pole R	0.3777	3.7289	**1.83E-03**	**−6.25E-05**	–	–	–	–	–	**−3.84E-01**	*−7.29E-02*	**1.57E-01**	3.86E-01	3.43E-01	–	–	–	–
Banks sts L	0.1674	2.4458	**−3.26E-03**	5.11E-06	−6.66E-07	*−2.04E-02*	**1.54E-07**	–	–	**−1.04E-01**	**−5.73E-02**	*2.35E-02*	**8.65E-02**	**4.62E-02**	–	–	−5.31E-08	**−1.08E-07**
Banks sts R	0.1780	2.5647	**−3.52E-03**	–	–	**−2.31E-02**	**1.23E-07**	−1.24E-13	–	**−1.69E-01**	**−7.55E-02**	−1.89E-02	**1.27E-01**	**1.35E-01**	–	−5.91E-04	−1.81E-08	*−8.94E-08*
Entorhinal L	0.3673	3.3172	**3.61E-03**	**−1.11E-04**	−1.89E-06	**6.91E-02**	1.35E-08	−2.65E-13	–	**−3.12E-01**	4.56E-02	3.39E-02	**1.73E-01**	**2.69E-01**	–	–	−3.90E-08	*−2.05E-07*
Entorhinal R	0.4100	3.5361	**3.67E-03**	**−1.42E-04**	–	3.79E-02	8.53E-08	**−4.91E-13**	–	**−4.33E-01**	−4.52E-02	−8.31E-03	**2.84E-01**	**3.94E-01**	–	–	−6.86E-08	**−3.59E-07**
Fusiform L	0.1642	2.6738	*−8.75E-04*	**−3.42E-05**	−8.44E-07	–	4.35E-08	–	–	**−2.27E-01**	**4.23E-02**	−5.97E-03	**1.00E-01**	**1.74E-01**	–	–	−1.09E-07	*−1.03E-07*
Fusiform R	0.1735	2.7110	−1.43E-04	*−3.12E-05*	−9.45E-07	−1.02E-02	**8.48E-08**	–	–	**−2.91E-01**	*3.48E-02*	**−5.57E-02**	**1.38E-01**	**2.48E-01**	–	*−7.70E-04*	*−1.54E-07*	**−1.23E-07**
Parahippocampal L	0.3202	2.7099	−3.14E-04	1.31E-05	−1.90E-06	–	*−1.59E-07*	−1.92E-13	8.62E-19	**−2.97E-01**	4.03E-02	**6.12E-02**	**1.47E-01**	**1.37E-01**	–	–	−1.72E-07	*−1.66E-07*
Parahippocampal R	0.2810	2.7238	5.33E-04	−5.87E-06	*−1.78E-06*	**−4.44E-02**	−1.54E-08	–	–	**−3.10E-01**	1.30E-03	2.21E-02	**1.63E-01**	**1.94E-01**	–	–	−1.59E-07	*−1.44E-07*
Superior frontal L	0.1525	2.6820	**−4.09E-03**	**6.53E-05**	**−2.15E-06**	**−4.92E-02**	−4.65E-08	−2.33E-14	*5.13E-19*	**−4.88E-02**	**−5.16E-02**	**−3.75E-02**	**7.42E-02**	**1.32E-01**	–	**−8.46E-04**	–	–
Superior frontal R	0.1533	2.6319	**−3.75E-03**	**6.89E-05**	**−2.21E-06**	**−5.27E-02**	–	–	–	**−2.37E-02**	−5.59E-03	**2.82E-02**	**5.59E-02**	**8.42E-02**	–	**−8.73E-04**	–	–
Rostral middle frontal L	0.1371	2.3418	**−3.11E-03**	**5.18E-05**	**−1.57E-06**	**−3.78E-02**	4.44E-09	1.22E-14	*4.13E-19*	**−3.42E-02**	−9.69E-03	**−4.49E-02**	2.81E-02	**1.09E-01**	–	−4.66E-04	**1.80E-07**	−1.65E-08
Rostral middle frontal R	0.1405	2.2536	**−2.61E-03**	**7.33E-05**	**−1.81E-06**	**−3.20E-02**	−1.90E-08	2.66E-14	3.62E-19	**2.82E-02**	1.03E-02	**3.68E-02**	1.15E-02	*3.00E-02*	–	*−6.24E-04*	–	–
Caudal middle frontal L	0.1477	2.5145	**−2.96E-03**	**5.57E-05**	**−1.67E-06**	**−4.93E-02**	5.57E-08	−1.85E-14	3.81E-19	**−5.37E-02**	**−3.76E-02**	**−8.22E-02**	*3.85E-02*	**1.35E-01**	–	*−6.25E-04*	–	–
Caudal middle frontal R	0.1507	2.4869	**−2.32E-03**	**6.20E-05**	**−2.17E-06**	**−6.23E-02**	**8.81E-08**	–	–	**−4.82E-02**	**−4.01E-02**	**−4.21E-02**	**6.36E-02**	**8.39E-02**	–	**−9.79E-04**	–	–

(continued on next page)

Table 4 *(continued)*

Region	RMSE	Int	Sociodemographics				Estimated total intracranial volume (eTIV)			Scanner			Interactions					
			Age	Age^2	Age^3	Sex	eTIV	$eTIV^2$	$eTIV^3$	Strength	Manufacturer		GE X MFS	Philips X MFS	eTIV X MFS	Age X Sex	eTIV X GE	eTIV X Philips
						M / F				1.5 T / 3 T	GE /Siemens	Philips /Siemens						
Pars opercularis L	0.1495	2.5310	**−4.10E-03**	**6.37E-05**	*−1.07E-06*	**−2.64E-02**	**1.02E-07**	–	–	**−6.69E-02**	**−3.86E-02**	4.08E-04	**6.04E-02**	*3.63E-02*	–	**−8.58E-04**	–	–
Pars opercularis R	0.1587	2.5184	**−3.71E-03**	**8.18E-05**	**−1.68E-06**	*−1.63E-02*	**6.98E-08**	–	–	**−6.74E-02**	**−6.02E-02**	1.48E-02	**9.55E-02**	*3.05E-02*	–	**−8.06E-04**	–	–
Pars triangularis L	0.1589	2.3956	**−4.88E-03**	**6.20E-05**	*−1.12E-06*	**−2.69E-02**	3.59E-08	–	–	**−4.04E-02**	*−3.38E-02*	*2.48E-02*	**6.13E-02**	2.00E-02	–	*−6.41E-04*	**1.62E-07**	2.06E-08
Pars triangularis R	0.1610	2.3760	**−5.20E-03**	**6.89E-05**	−8.99E-07	**−2.67E-02**	8.62E-09	–	–	7.82E-03	*−2.83E-02*	**8.15E-02**	2.31E-02	**−4.92E-02**	–	–	**1.57E-07**	1.55E-08
Pars orbitalis L	0.2216	2.6675	**−3.36E-03**	**8.14E-05**	**−1.81E-06**	**−4.07E-02**	*−1.06E-07*	−1.91E-14	*6.63E-19*	**−9.03E-02**	−1.84E-02	*3.59E-02*	**9.97E-02**	**1.28E-01**	–	**−1.15E-03**	–	–
Pars orbitalis R	0.2201	2.6441	**−2.44E-03**	**5.56E-05**	**−2.16E-06**	**−5.28E-02**	5.23E-09	−1.64E-13	–	**−4.19E-02**	1.39E-02	**5.53E-02**	**7.78E-02**	**9.00E-02**	–	**−1.56E-03**	–	–
Lateral orbitofrontal L	0.1713	2.5736	**−2.18E-03**	**4.90E-05**	*−1.41E-06*	−2.88E-03	*−9.33E-08*	−6.84E-14	*6.37E-19*	**−1.31E-01**	**8.27E-02**	**1.10E-01**	*4.52E-02*	**7.62E-02**	*1.07E-07*	**−1.35E-03**	−1.58E-08	**−1.17E-07**
Lateral orbitofrontal R	0.1782	2.5310	**−2.38E-03**	**4.91E-05**	*−1.33E-06*	−9.91E-03	**−1.29E-07**	−1.02E-13	**9.42E-19**	**−3.46E-02**	**8.96E-02**	**1.10E-01**	–	–	6.06E-08	**−1.23E-03**	–	–
Medial orbitofrontal L	0.1663	2.3366	**−2.71E-03**	**4.98E-05**	−8.59E-07	*1.93E-02*	−5.93E-08	−4.46E-15	**7.18E-19**	*−2.16E-02*	**1.06E-01**	*2.44E-02*	*−5.06E-02*	*3.91E-02*	–	**−1.08E-03**	–	–
Medial orbitofrontal R	0.1773	2.2885	**−2.76E-03**	**8.72E-05**	**−1.80E-06**	–	**−1.11E-07**	3.44E-14	*6.30E-19*	−2.63E-03	**1.30E-01**	**1.63E-01**	*−5.05E-02*	**−6.38E-02**	–	–	–	–
Precentral L	0.1470	2.5165	**−2.70E-03**	**2.78E-05**	**−1.52E-06**	**−4.05E-02**	4.85E-08	**−1.74E-13**	–	**−9.74E-02**	*−2.53E-02*	**−6.76E-02**	−2.72E-02	**7.65E-02**	–	*−6.93E-04*	**1.75E-07**	−7.50E-09
Precentral R	0.1454	2.4834	**−2.69E-03**	1.33E-05	*−1.18E-06*	**−4.46E-02**	2.51E-08	**−1.75E-13**	–	**−7.77E-02**	−2.26E-02	**−5.08E-02**	−9.86E-03	**4.19E-02**	–	*−6.93E-04*	**1.54E-07**	7.77E-09
Paracentral L	0.1601	2.3228	**−2.74E-03**	**5.10E-05**	**−1.77E-06**	**−3.38E-02**	3.03E-09	−2.02E-14	2.80E-19	**−6.01E-02**	−1.67E-02	**−1.12E-01**	−1.92E-02	**8.14E-02**	–	–	**2.05E-07**	7.08E-08
Paracentral R	0.1531	2.3633	**−2.58E-03**	**5.09E-05**	**−1.56E-06**	**−3.02E-02**	*6.20E-08*	–	–	**−1.14E-01**	**−4.64E-02**	**−1.54E-01**	1.05E-02	**1.28E-01**	–	*−6.33E-04*	**1.98E-07**	−3.69E-09
Frontal pole L	0.2867	2.7339	**−4.16E-03**	*4.18E-05*	–	*−3.01E-02*	*−1.37E-07*	−1.15E-13	*8.45E-19*	3.03E-02	9.08E-03	−1.48E-02	−6.05E-02	**8.26E-02**	–	–	–	–
Frontal pole R	0.2821	2.6940	**−3.61E-03**	**7.21E-05**	–	**−7.29E-02**	–	–	–	**4.11E-02**	1.76E-02	**7.87E-02**	–	–	–	*−1.06E-03*	–	–
Postcentral L	0.1259	2.0856	**−2.23E-03**	2.61E-06	*−9.65E-07*	**−4.90E-02**	**1.04E-07**	–	–	**−3.88E-02**	**−3.91E-02**	**−1.03E-01**	−2.65E-02	**7.09E-02**	–	−4.33E-04	6.94E-08	2.77E-09
Postcentral R	0.1295	2.0646	**−2.37E-03**	−3.41E-06	*−8.54E-07*	**−5.06E-02**	**1.23E-07**	–	–	**−4.77E-02**	**−4.74E-02**	**−1.01E-01**	4.73E-03	**6.74E-02**	–	–	–	–
Supramarginal L	0.1416	2.5271	**−3.22E-03**	4.08E-06	**−1.56E-06**	**−4.81E-02**	**9.03E-08**	–	–	**−6.48E-02**	**−7.07E-02**	**−2.94E-02**	**6.98E-02**	**7.01E-02**	−5.08E-08	−4.63E-04	4.36E-08	−5.94E-08
Supramarginal R	0.1479	2.5458	**−3.42E-03**	5.76E-07	*−1.16E-06*	**−4.30E-02**	**8.75E-08**	−1.15E-13	–	**−8.26E-02**	**−7.92E-02**	**−6.85E-02**	**8.95E-02**	**9.79E-02**	–	−5.17E-04	1.97E-08	−5.14E-08
Superior parietal L	0.1280	2.1852	**−1.70E-03**	3.66E-06	**−1.89E-06**	**−4.89E-02**	**9.82E-08**	–	–	**−5.51E-02**	**−4.41E-02**	**−1.29E-01**	−6.93E-03	**1.12E-01**	–	–	–	–
Superior parietal R	0.1292	2.1801	**−1.78E-03**	−5.98E-06	**−1.76E-06**	**−5.30E-02**	**1.23E-07**	–	–	**−3.96E-02**	−1.95E-02	**−1.38E-01**	**−4.05E-02**	**9.92E-02**	*−5.99E-08*	−3.45E-04	–	–
Inferior parietal L	0.1371	2.4192	**−2.79E-03**	−7.41E-06	**−1.78E-06**	**−4.48E-02**	6.14E-08	3.69E-14	3.38E-19	**−6.31E-02**	**−5.65E-02**	**−5.32E-02**	**5.96E-02**	**9.18E-02**	−5.16E-08	–	–	–
Inferior parietal R	0.1369	2.4624	**−3.12E-03**	−1.42E-05	**−1.45E-06**	**−4.14E-02**	3.85E-08	3.68E-14	3.37E-19	**−9.26E-02**	**−6.77E-02**	**−1.04E-01**	**6.54E-02**	**1.42E-01**	*−6.45E-08*	–	–	–

(continued on next page)

Table 4 *(continued)*

Region	RMSE	Int	Sociodemographics				Estimated total intracranial volume (eTIV)			Scanner			Interactions					
			Age	Age^2	Age^3	Sex	eTIV	$eTIV^2$	$eTIV^3$	Strength	Manufacturer		GE X MFS	Philips X MFS	eTIV X MFS	Age X Sex	eTIV X GE	eTIV X Philips
						M / F				1.5 T / 3 T	GE /Siemens	Philips /Siemens						
Precuneus L	0.1366	2.3399	**−2.91E-03**	9.10E-06	**−1.71E-06**	**−3.06E-02**	**8.92E-08**	–	–	**−7.82E-02**	−2.05E-02	**−7.52E-02**	3.53E-03	**9.35E-02**	–	**−7.16E-04**	2.36E-08	−4.78E-08
Precuneus R	0.1312	2.3575	**−2.85E-03**	1.11E-05	**−1.66E-06**	**−3.54E-02**	**8.25E-08**	–	–	**−6.61E-02**	2.15E-02	**−7.70E-02**	**−6.86E-02**	**7.33E-02**	–	**−6.88E-04**	*1.11E-07*	−3.95E-08
Lingual L	0.1365	1.9499	**−2.97E-03**	1.29E-05	*−1.02E-06*	*−1.49E-02*	**5.34E-08**	–	–	1.42E-02	**6.90E-02**	**−1.11E-01**	**−1.07E-01**	2.31E-02	–	*−5.32E-04*	–	–
Lingual R	0.1403	1.9995	**−3.40E-03**	8.63E-06	−7.16E-07	−1.27E-02	2.22E-08	*1.32E-13*	3.20E-19	**2.65E-02**	**5.99E-02**	**−1.32E-01**	**−1.42E-01**	−1.52E-02	5.88E-08	–	−1.31E-08	*−7.68E-08*
Pericalcarine L	0.1658	1.5618	**−3.51E-03**	**3.27E-05**	–	−1.44E-02	2.68E-08	*1.84E-13*	4.02E-19	**9.04E-02**	**5.79E-02**	**−1.52E-01**	**−2.16E-01**	−3.07E-02	–	–	–	–
Pericalcarine R	0.1631	1.5635	**−2.51E-03**	**5.72E-05**	**−1.33E-06**	–	−1.30E-09	*1.70E-13*	**6.09E-19**	**7.39E-02**	7.53E-03	**−1.59E-01**	**−1.67E-01**	*−3.81E-02*	–	–	–	–
Cuneus L	0.1517	1.7967	**−2.33E-03**	**4.29E-05**	**−1.26E-06**	**−2.89E-02**	**7.71E-08**	–	–	**3.99E-02**	**4.95E-02**	**−1.11E-01**	**−1.33E-01**	1.15E-02	–	–	–	–
Cuneus R	0.1462	1.8327	**−2.41E-03**	**3.49E-05**	**−1.19E-06**	**−2.71E-02**	4.51E-08	4.50E-14	3.24E-19	**5.00E-02**	8.88E-03	**−1.32E-01**	**−1.36E-01**	−1.71E-02	–	–	–	–
Lateral occipital L	0.1288	2.1672	**−1.06E-03**	**−4.93E-05**	**−1.61E-06**	**−3.28E-02**	**4.89E-08**	–	–	**−3.80E-02**	−7.09E-03	**−9.22E-02**	−1.92E-02	**6.56E-02**	–	–	–	–
Lateral occipital R	0.1343	2.2242	**−1.19E-03**	**−5.48E-05**	**−1.32E-06**	**−3.20E-02**	**1.01E-07**	–	–	**−4.67E-02**	*2.24E-02*	**−1.11E-01**	**−6.46E-02**	**8.45E-02**	–	–	−6.48E-08	−6.03E-08
Rostral anterior cingulate L	0.2499	2.7778	**−1.48E-03**	**1.03E-04**	–	−7.00E-03	**−2.17E-07**	8.34E-14	**9.94E-19**	**−2.13E-01**	**8.72E-02**	**7.17E-02**	**9.09E-02**	**1.82E-01**	–	**−1.78E-03**	–	–
Rostral anterior cingulate R	0.2544	2.6610	**−1.74E-03**	**1.04E-04**	−9.68E-07	2.10E-02	**−1.73E-07**	1.22E-13	6.08E-19	**−9.48E-02**	**1.15E-01**	**1.70E-01**	**8.70E-02**	**6.91E-02**	–	–	–	–
Caudal anterior cingulate L	0.2700	2.6007	−3.10E-04	**1.16E-04**	–	**−3.74E-02**	*−9.35E-08*	–	–	**−2.02E-01**	3.52E-02	−2.62E-03	**1.23E-01**	**2.19E-01**	–	*−1.09E-03*	–	–
Caudal anterior cingulate R	0.2454	2.4328	−4.92E-04	**1.29E-04**	**−2.51E-06**	–	**−2.89E-07**	−1.47E-14	*8.65E-19*	**−9.67E-02**	**1.33E-01**	**7.09E-02**	3.61E-02	**6.66E-02**	*1.22E-07*	–	–	–
Posterior cingulate L	0.1622	2.4490	**−2.43E-03**	**6.40E-05**	**−1.71E-06**	−1.03E-02	–	–	–	**−1.19E-01**	**9.64E-02**	5.60E-04	−9.66E-03	**8.86E-02**	–	**−8.25E-04**	–	–
Posterior cingulate R	0.1582	2.4045	**−3.01E-03**	**7.11E-05**	−8.29E-07	**−2.41E-02**	–	–	–	**−8.84E-02**	**1.42E-01**	**3.18E-02**	*−3.99E-02*	**4.77E-02**	–	**−1.12E-03**	–	–
Isthmus cingulate L	0.2084	2.4181	**−3.57E-03**	1.49E-05	−9.38E-07	2.54E-03	**−1.18E-07**	–	–	**−9.68E-02**	**8.90E-02**	1.07E-02	−3.76E-02	**5.19E-02**	–	*−7.85E-04*	–	–
Isthmus cingulate R	0.1953	2.3472	**−2.86E-03**	**3.95E-05**	**−1.80E-06**	−9.52E-03	**−1.80E-07**	5.92E-14	*5.70E-19*	**−5.66E-02**	**1.20E-01**	2.39E-03	*−4.86E-02*	1.18E-02	–	**−1.33E-03**	–	–
Insula L	0.1771	2.9713	**−2.76E-03**	**3.04E-05**	–	8.96E-03	−8.17E-09	−1.36E-13	*5.87E-19*	**−1.28E-01**	1.53E-02	−1.54E-02	**9.83E-02**	**1.75E-01**	*1.09E-07*	**−1.02E-03**	8.52E-08	**−1.39E-07**
Insula R	0.1885	2.9534	**−2.67E-03**	**3.81E-05**	–	2.02E-03	−3.41E-08	−4.33E-14	**8.20E-19**	**−1.38E-01**	−1.48E-02	−9.87E-03	**1.31E-01**	**1.41E-01**	*9.24E-08*	**−9.67E-04**	6.73E-08	*−1.01E-07*
Cortex L	0.1022	2.4415	**−1.93E-03**	*2.66E-05*	−2.07E-06	**−3.02E-02**	**1.92E-08**	**−2.46E-14**	4.71E-19	−7.49E-02	**−3.77E-02**	−4.06E-02	*2.10E-02*	9.60E-02	–	−4.62E-04	–	–
Cortex R	0.1003	2.4363	**−1.82E-03**	**2.49E-05**	**−1.94E-06**	−2.88E-02	**8.57E-09**	**−8.13E-14**	*3.87E-19*	**−7.21E-02**	**−4.80E-02**	−3.42E-02	**3.32E-02**	8.88E-02	–	−4.85E-04	–	–

Note. Categories are coded 0 and 1 with reference categories (Female, Siemens, and 3 T) coded 0. Age and eTIV are centered by the mean (Age – 47.58; eTIV – 1528926.15). Int: Intercept. RMSE: Root mean square error. STS: Superior temporal sulcus.

Italic $p < .05$; **Bold** $p < .01$.

Table 5
Coefficients of models predicting left (L) and right (R) regional cortical volume.

Region	RMSE	Int	Sociodemographics				Estimated total intracranial volume (eTIV)			Scanner			Interactions					
			Age	Age^2	Age^3	Sex	eTIV	$eTIV^2$	$eTIV^3$	Strength	Manufacturer		GE X MFS	Philips X MFS	eTIV X MFS	Age X Sex	eTIV X GE	eTIV X Philips
						M / F				1.5 T / 3 T	GE/ Siemens	Philips/ Siemens						
Superior temporal L	1169.17	11608.9	**−2.76E+01**	4.78E-02	*−9.27E-03*	**2.10E+02**	**5.48E-03**	**1.97E-09**	–	**−2.25E+02**	**−2.72E+02**	**−3.61E+02**	–	–	–	**−8.90E+00**	−7.57E-04	−5.41E-04
Superior temporal R	1061.54	11201.6	**−3.06E+01**	*1.64E-01*	*−7.29E-03*	−3.93E+01	**5.18E-03**	**2.38E-09**	–	**−2.16E+02**	**−2.47E+02**	**−1.90E+02**	–	–	–	−3.56E+00	−3.94E-04	*−6.17E-04*
Middle temporal L	1167.03	10520.1	**−2.57E+01**	2.78E-02	*−7.69E-03*	*1.41E+02*	**6.03E-03**	4.04E-10	−3.40E-15	**−5.99E+01**	−1.22E+02	**−5.05E+02**	1.75E+02	**6.23E+02**	–	**−7.30E+00**	−4.44E-04	−1.24E-03
Middle temporal R	1213.54	11605.8	**−2.93E+01**	*1.73E-01*	*−8.69E-03*	9.81E+01	**6.62E-03**	9.13E-10	**−5.08E-15**	**−5.23E+02**	5.36E+01	**−2.95E+02**	−1.35E+02	**4.13E+02**	–	**−7.23E+00**	6.50E-04	**−8.70E-04**
Inferior temporal L	1297.75	10365.6	**−2.45E+01**	−1.23E-01	–	1.20E+02	**5.84E-03**	**1.92E-09**	−1.73E-15	−1.25E+02	**4.28E+02**	**−2.77E+02**	**−5.12E+02**	*3.11E+02*	–	–	−1.07E-04	−5.70E-04
Inferior temporal R	1317.18	10320.4	**−1.11E+01**	−1.29E-02	**−1.16E-02**	1.02E+02	**5.95E-03**	–	–	**−6.81E+02**	−3.24E+01	**−3.89E+02**	1.52E+02	8.32E+02	–	−4.83E+00	−4.39E-04	**−9.35E-04**
Transverse temporal L	202.43	1155.7	**−2.36E+00**	**4.00E-02**	**−1.88E-03**	−1.64E+01	**5.84E-04**	*1.75E-10*	−4.15E-16	*2.35E+01*	−2.83E+01	**−6.37E+01**	**−6.99E+01**	−3.35E+01	–	–	–	–
Transverse temporal R	154.07	899.7	**−1.73E+00**	−1.83E-03	*−1.12E-03*	−1.27E+01	**4.81E-04**	*1.50E-10*	−4.43E-16	−4.74E+00	2.62E+00	**−4.81E+01**	−3.39E+01	−2.28E+00	–	–	–	–
Temporal pole L	375.91	2395.8	*−1.36E+00*	3.64E-02	–	**6.64E+01**	**4.73E-04**	*−3.52E-10*	1.10E-15	**−8.50E+01**	**8.02E+01**	**1.41E+02**	–	–	–	**−2.01E+00**	2.74E-04	−8.22E-05
Temporal pole R	375.65	2263.4	4.28E-02	–	–	2.76E+01	**5.34E-04**	–	–	**−2.52E+02**	2.57E+01	2.98E+01	**2.22E+02**	**2.02E+02**	–	−1.32E+00	–	–
Banks sts L	401.76	2481.4	**−7.66E+00**	–	–	**5.76E+01**	**1.27E-03**	**5.02E-10**	–	**−8.23E+01**	**−8.79E+01**	**−7.03E+01**	–	–	–	−1.08E+00	−1.18E-04	−1.86E-04
Banks sts R	351.83	2350.4	**−5.46E+00**	1.70E-02	*−2.27E-03*	2.54E+01	**1.12E-03**	1.57E-10	−8.92E-16	**−1.31E+02**	**−1.41E+02**	**−1.02E+02**	5.88E+01	**8.69E+01**	–	–	–	–
Entorhinal L	323.94	1790.6	**4.75E+00**	**−1.08E-01**	**−3.35E-03**	**1.18E+02**	**7.90E-04**	–	–	**−1.11E+02**	1.42E+01	8.81E+00	**1.28E+02**	**1.79E+02**	*1.57E-04*	−1.12E+00	6.97E-05	**−2.40E-04**
Entorhinal R	333.57	1757.3	**4.28E+00**	**−8.56E-02**	−1.84E-03	**5.92E+01**	**9.13E-04**	–	–	**−2.57E+02**	**−8.74E+01**	**−1.52E+02**	**2.50E+02**	**3.15E+02**	1.38E-04	–	−1.11E-04	**−4.41E-04**
Fusiform L	1183.14	9885.1	**−1.43E+01**	6.37E-03	*−9.84E-03*	**1.98E+02**	**5.12E-03**	3.24E-10	*−4.19E-15*	**−7.31E+02**	−6.39E+01	**−4.93E+02**	1.42E+02	**5.67E+02**	–	*−4.73E+00*	−7.95E-04	**−9.86E-04**
Fusiform R	1132.33	9668.5	**−1.10E+01**	−1.35E-01	−6.84E-03	**3.70E+02**	**4.41E-03**	*1.23E-09*	–	**−1.18E+03**	−6.00E+01	**−7.61E+02**	*3.61E+02*	**9.85E+02**	–	**−6.46E+00**	−1.06E-05	**−8.08E-04**
Parahippocampal L	313.89	2222.9	**−2.42E+00**	−2.11E-02	**−2.94E-03**	1.96E+01	**7.86E-04**	*2.90E-10*	–	**−2.16E+02**	−1.69E+01	*−4.46E+01*	*8.94E+01*	5.70E+01	*−1.60E-04*	–	–	–
Parahippocampal R	283.43	2117.7	**−3.48E+00**	**−5.97E-02**	–	–	**8.43E-04**	2.23E-10	–	**−2.38E+02**	−3.67E+01	*−4.89E+01*	**1.27E+02**	**8.72E+01**	−1.02E-04	–	1.15E-04	−1.09E-04
Superior frontal L	1800.60	21459.8	**−7.36E+01**	**9.22E-01**	**−1.73E-02**	7.23E+01	**1.02E-02**	**4.37E-09**	−4.25E-15	1.61E+01	**−5.71E+02**	**−9.62E+02**	**−6.13E+02**	1.09E+02	–	**−1.12E+01**	–	–
Superior frontal R	1838.56	20649.9	**−6.85E+01**	**8.43E-01**	**−1.54E-02**	1.51E+01	**1.05E-02**	**3.79E-09**	**−7.53E-15**	−2.11E+01	**−5.04E+02**	**−6.34E+02**	−3.53E+02	5.38E+00	–	**−1.30E+01**	–	–
Rostral middle frontal L	1528.06	14844.0	**−5.86E+01**	**7.38E-01**	−9.51E-03	5.37E+01	**8.00E-03**	**2.90E-09**	–	−1.60E+02	1.10E+02	**−8.00E+02**	**−5.07E+02**	*3.29E+02*	–	−5.48E+00	*1.14E-03*	*−9.51E-04*
Rostral middle frontal R	1609.29	14852.2	**−5.62E+01**	**8.89E-01**	**−1.51E-02**	1.41E+02	**7.75E-03**	**4.31E-09**	–	4.05E+01	2.03E+02	**−3.05E+02**	**−6.24E+02**	−3.78E+01	–	–	–	–
Caudal middle frontal L	940.54	6198.9	**−1.96E+01**	**2.79E-01**	**−8.06E-03**	–	**3.55E-03**	**1.36E-09**	–	*−1.33E+02*	−1.37E+02	**−3.43E+02**	−1.95E+02	*1.86E+02*	–	–	3.77E-04	*−5.46E-04*
Caudal middle frontal R	918.45	5834.4	**−1.78E+01**	**2.21E-01**	−5.67E-03	**−1.84E+02**	**4.30E-03**	7.91E-10	**−5.01E-15**	−7.58E+01	−7.00E+01	**−2.23E+02**	–	–	–	*−4.29E+00*	4.28E-04	**−6.05E-04**

(continued on next page)

Table 5 *(continued)*

Region	RMSE	Int	Sociodemographics				Estimated total intracranial volume (eTIV)			Scanner			Interactions					
			Age	Age^2	Age^3	Sex	eTIV	$eTIV^2$	$eTIV^3$	Strength	Manufacturer		GE X MFS	Philips X MFS	eTIV X MFS	Age X Sex	eTIV X GE	eTIV X Philips
						M / F				1.5 T / 3 T	GE/ Siemens	Philips/ Siemens						
Pars opercularis L	690.59	4666.6	**−1.82E+01**	**1.72E-01**	–	−1.28E+01	**2.35E-03**	*7.26E-10*	–	*−9.42E+01*	−1.43E+01	**−1.74E+02**	**−2.39E+02**	−1.76E+01	–	**−4.94E+00**	3.26E-04	−2.78E-04
Pars opercularis R	566.81	3882.8	**−1.54E+01**	**9.66E-02**	–	1.27E+01	**2.01E-03**	1.63E-10	**−2.71E-15**	–	**−1.81E+02**	**−1.86E+02**	–	–	–	**−2.77E+00**	–	–
Pars triangularis L	505.73	3388.8	**−1.41E+01**	**1.73E-01**	−2.09E-03	**7.58E+01**	**1.43E-03**	**6.78E-10**	−1.22E-15	**−6.37E+01**	**−8.05E+01**	**−1.46E+02**	–	–	–	**−2.85E+00**	–	–
Pars triangularis R	616.04	3902.5	**−1.91E+01**	**2.01E-01**	–	**1.27E+02**	**1.34E-03**	*6.65E-10*	–	3.57E+01	−5.59E+01	*−8.76E+01*	**−1.99E+02**	*−1.28E+02*	2.73E-04	**−3.12E+00**	–	–
Pars orbitalis L	284.34	2110.9	**−5.38E+00**	**9.53E-02**	**−2.66E-03**	1.64E+01	**8.54E-04**	–	–	**−1.12E+02**	−1.93E+01	*−4.63E+01*	3.50E+01	**9.61E+01**	−6.36E-05	**−1.88E+00**	–	–
Pars orbitalis R	331.87	2482.6	**−6.13E+00**	**1.34E-01**	**−3.36E-03**	**6.20E+01**	**8.49E-04**	1.29E-11	6.64E-16	**−8.97E+01**	1.77E+01	*−5.84E+01*	−2.07E+01	**8.89E+01**	–	**−2.67E+00**	2.13E-04	−1.12E-04
Lateral orbitofrontal L	675.37	7297.5	**−1.60E+01**	**2.22E-01**	**−6.23E-03**	5.14E+01	**3.38E-03**	*7.51E-10*	–	**−5.05E+02**	−4.75E+00	**−1.80E+02**	−1.28E+01	**4.36E+02**	–	**−4.41E+00**	4.45E-04	−2.44E-04
Lateral orbitofrontal R	672.23	7026.3	**−1.81E+01**	**1.86E-01**	*−4.69E-03*	1.54E+01	**3.13E-03**	–	–	*7.73E+01*	**2.89E+02**	−3.21E+01	**−5.62E+02**	−1.06E+02	–	**−4.78E+00**	**6.52E-04**	−4.38E-05
Medial orbitofrontal L	546.33	4806.5	**−1.26E+01**	6.25E-02	–	**9.56E+01**	**2.46E-03**	**7.47E-10**	–	**1.49E+02**	**4.04E+02**	**−1.94E+02**	**−5.06E+02**	−4.28E+01	–	**−3.22E+00**	–	–
Medial orbitofrontal R	506.17	4832.3	**−1.21E+01**	**2.38E-01**	**−4.72E-03**	**8.19E+01**	**1.96E-03**	–	–	−4.93E+01	**2.44E+02**	−3.09E+01	**−3.22E+02**	**−1.54E+02**	–	−1.87E+00	–	–
Precentral L	1285.93	12991.4	**−2.81E+01**	**3.42E-01**	*−1.05E-02*	**2.17E+02**	**4.85E-03**	–	–	**−3.66E+02**	**−3.94E+02**	**−8.34E+02**	*−3.54E+02*	1.94E+02	–	**−8.25E+00**	**1.70E-03**	−1.59E-04
Precentral R	1245.71	12879.5	**−3.12E+01**	–	–	**1.68E+02**	**5.15E-03**	*1.33E-09*	–	*−1.61E+02*	**−3.27E+02**	**−6.21E+02**	**−4.38E+02**	−1.78E+02	–	**−8.96E+00**	*1.03E-03*	−4.28E-04
Paracentral L	478.30	3384.1	**−7.15E+00**	6.45E-02	−2.89E-03	−3.64E+01	**1.52E-03**	**6.28E-10**	−9.89E-16	−9.30E+00	**−1.28E+02**	**−3.02E+02**	**−1.54E+02**	3.71E+01	–	−1.48E+00	*3.96E-04*	5.18E-05
Paracentral R	544.38	3856.5	**−1.10E+01**	–	–	–	**1.72E-03**	**7.77E-10**	–	**−8.21E+01**	**−2.43E+02**	**−3.27E+02**	–	–	–	–	–	–
Frontal pole L	146.85	736.0	**−1.92E+00**	**7.79E-02**	*−1.13E-03*	4.98E+00	**2.15E-04**	1.12E-10	–	**2.35E+01**	2.15E+01	−1.75E+01	**−7.26E+01**	*−2.92E+01*	–	*−5.78E-01*	–	–
Frontal pole R	184.70	970.1	**−3.62E+00**	**1.02E-01**	–	1.63E+01	**2.64E-04**	1.39E-10	–	**4.98E+01**	**6.46E+01**	9.62E+00	**−1.12E+02**	**−7.40E+01**	–	**−8.95E-01**	–	–
Postcentral L	1083.68	9647.0	**−2.01E+01**	*1.88E-01*	*−7.35E-03*	−2.83E+01	**4.63E-03**	3.34E-10	*−3.91E-15*	**−1.63E+02**	**−5.14E+02**	**−7.10E+02**	−2.16E+02	5.20E+01	–	−3.92E+00	–	–
Postcentral R	1062.14	9086.2	**−2.03E+01**	*1.51E-01*	−5.92E-03	−9.89E+01	**4.31E-03**	7.53E-10	−2.19E-15	**−1.73E+02**	**−4.36E+02**	**−6.21E+02**	–	–	–	–	–	–
Supramarginal L	1240.60	10587.7	**−2.70E+01**	1.66E-01	*−8.00E-03*	1.03E+02	**6.13E-03**	*1.34E-09*	**−7.79E-15**	**−2.94E+02**	**−3.69E+02**	**−3.41E+02**	–	–	−3.69E-04	*−4.73E+00*	–	–
Supramarginal R	1188.83	10091.6	**−2.55E+01**	*1.82E-01*	*−7.71E-03*	−6.65E+01	**5.12E-03**	**1.43E-09**	*−3.78E-15*	**−1.75E+02**	**−3.79E+02**	**−4.80E+02**	–	–	–	**−7.84E+00**	–	–
Superior parietal L	1354.03	12992.4	**−2.88E+01**	−8.07E-02	−7.40E-03	**−2.78E+02**	**6.36E-03**	**1.96E-09**	**−5.25E-15**	**−3.45E+02**	*−2.75E+02*	**−9.60E+02**	*−4.19E+02*	**4.91E+02**	–	−4.71E+00	–	–
Superior parietal R	1340.43	13068.0	**−3.39E+01**	**−2.21E-01**	–	**−2.35E+02**	**6.45E-03**	**1.88E-09**	**−6.07E-15**	**−2.81E+02**	*−2.30E+02*	**−1.09E+03**	**−5.07E+02**	**4.44E+02**	−4.25E-04	**−6.87E+00**	–	–
Inferior parietal L	1448.35	12083.7	**−2.74E+01**	**3.10E-01**	**−1.75E-02**	2.66E+01	**5.81E-03**	*1.32E-09*	–	**−3.84E+02**	**−5.55E+02**	**−6.89E+02**	*3.56E+02*	**4.52E+02**	–	**−1.07E+01**	8.85E-04	−5.08E-04
Inferior parietal R	1628.43	14453.5	**−3.81E+01**	2.08E-01	**−1.57E-02**	**3.57E+02**	**6.55E-03**	**2.11E-09**	–	**−6.87E+02**	**−6.01E+02**	**−1.11E+03**	−2.76E+00	**7.81E+02**	–	**−8.35E+00**	8.59E-04	**−1.06E-03**
Precuneus L	918.86	9337.9	**−2.50E**	**2.21E-**	*−6.87E-*	4.85E+01	**5.02E-**	**1.45E-**	*−3.11E-*	**−2.73E**	**−3.12E**	**−5.49E**	*−2.86E*	*1.92E+02*	*−4.38E-*	**−6.74E**	5.68E-	−3.73E-

(continued on next page)

Table 5 *(continued)*

Region	RMSE	Int	Sociodemographics				Estimated total intracranial volume (eTIV)			Scanner			Interactions					
			Age	Age^2	Age^3	Sex	eTIV	$eTIV^2$	$eTIV^3$	Strength	Manufacturer		GE X MFS	Philips X MFS	eTIV X MFS	Age X Sex	eTIV X GE	eTIV X Philips
						M / F				1.5 T / 3 T	GE/ Siemens	Philips/ Siemens						
			+01	**01**	*03*		**03**	**09**	*15*	**+02**	**+02**	**+02**	*+02*		*04*	**+00**	04	04
Precuneus R	972.29	9674.5	**−2.50E +01**	**2.82E-01**	**−8.21E-03**	**1.26E +02**	**4.75E-03**	**1.69E-09**	–	**−2.18E +02**	**−2.21E +02**	**−5.96E +02**	**−5.39E +02**	1.74E+02	–	**−6.67E +00**	*7.71E-04*	*−5.90E-04*
Lingual L	904.39	6394.8	**−1.20E +01**	2.12E-02	**−8.04E-03**	**1.28E +02**	**2.84E-03**	*9.46E-10*	−2.04E-15	*−1.16E +02*	−3.01E+00	**−7.54E +02**	*−2.34E +02*	1.57E+02	–	**−5.37E +00**	3.02E-05	**−7.47E-04**
Lingual R	880.97	6607.2	**−1.33E +01**	2.38E-02	*−7.13E-03*	**1.32E +02**	**2.59E-03**	**1.19E-09**	–	1.64E+01	−8.84E+01	**−8.37E +02**	**−4.71E +02**	6.03E+00	–	**−4.32E +00**	−6.29E-05	**−8.84E-04**
Pericalcarine L	385.23	1970.5	**−6.44E +00**	**7.61E-02**	–	–	**8.48E-04**	**8.60E-10**	6.98E-16	1.80E+01	−1.49E+01	**−2.76E +02**	**−1.78E +02**	5.73E+01	–	–	–	–
Pericalcarine R	418.93	2216.7	**−4.58E +00**	**8.46E-02**	−2.54E-03	*4.19E+01*	**1.07E-03**	**8.93E-10**	–	3.81E+01	*−8.77E+01*	**−3.34E +02**	**−1.92E +02**	4.01E+01	−1.85E-04	–	–	–
Cuneus L	440.72	2791.5	**−7.04E +00**	5.64E-02	−2.68E-03	3.62E+01	**1.08E-03**	**7.48E-10**	–	–	**−1.22E +02**	**−2.45E +02**	–	–	–	–	–	–
Cuneus R	452.96	2990.3	**−7.63E +00**	2.87E-02	−2.13E-03	2.85E+01	**1.48E-03**	**6.38E-10**	−5.80E-16	**1.35E +02**	−6.34E+01	**−2.94E +02**	**−3.26E +02**	*−9.11E +01*	−1.68E-04	–	–	–
Lateral occipital L	1292.70	11134.0	**−1.49E +01**	*−2.05E-01*	**−1.19E-02**	**3.04E +02**	**4.69E-03**	**1.94E-09**	–	**−2.45E +02**	−1.03E+02	**−9.31E +02**	*−3.88E +02*	**4.03E +02**	–	−4.39E +00	2.71E-04	**−8.95E-04**
Lateral occipital R	1315.51	11099.9	**−2.62E +01**	**−2.96E-01**	–	**3.98E +02**	**5.11E-03**	**1.53E-09**	–	−1.18E +02	−1.17E+02	**−8.32E +02**	**−5.69E +02**	*2.91E+02*	–	–	−5.84E-04	**−1.26E-03**
Rostral anterior cingulate L	423.40	2628.5	**−4.73E +00**	**9.83E-02**	–	–	**1.64E-03**	**7.42E-10**	–	**−2.25E +02**	**−9.46E +01**	−4.22E+01	7.47E+01	**1.57E +02**	−1.09E-04	–	–	–
Rostral anterior cingulate R	394.02	2086.8	**−4.29E +00**	**6.40E-02**	–	2.39E+01	**1.26E-03**	**7.91E-10**	–	**−1.13E +02**	–	–	–	–	–	–	–	–
Caudal anterior cingulate L	432.45	1824.6	−2.13E +00	**9.81E-02**	−1.95E-03	*−5.12E +01*	**9.71E-04**	**5.58E-10**	–	**−1.46E +02**	**−1.38E +02**	**−8.20E +01**	**1.95E +02**	**1.43E +02**	–	−1.14E +00	–	–
Caudal anterior cingulate R	460.28	2117.8	*−2.73E +00*	**1.28E-01**	**−4.06E-03**	–	**9.52E-04**	–	–	**−1.08E +02**	−2.40E+01	*−7.01E+01*	−1.19E +01	*1.06E+02*	–	–	–	–
Posterior cingulate L	422.88	3051.7	**−6.89E +00**	**1.59E-01**	**−3.55E-03**	**6.49E +01**	**1.45E-03**	1.95E-10	−1.24E-15	**−1.77E +02**	**−1.51E +02**	**−1.54E +02**	8.76E+01	*8.76E+01*	–	**−2.92E +00**	–	–
Posterior cingulate R	421.02	3107.2	**−7.68E +00**	**1.10E-01**	*−2.74E-03*	3.27E+01	**1.54E-03**	**5.16E-10**	–	**−1.24E +02**	*−7.23E+01*	**−1.31E +02**	*−1.19E +02*	7.87E+01	–	*−1.73E +00*	–	–
Isthmus cingulate L	366.44	2551.4	**−4.91E +00**	**8.65E-02**	*−2.34E-03*	**9.27E +01**	**1.48E-03**	1.53E-10	**−1.68E-15**	**−8.96E +01**	**−8.95E +01**	**−1.72E +02**	−7.46E +01	3.19E+01	–	*−1.74E +00*	–	–
Isthmus cingulate R	352.14	2372.0	**−6.44E +00**	3.97E-02	–	**4.74E +01**	**1.31E-03**	**7.97E-10**	–	–	**−8.93E +01**	**−1.86E +02**	–	–	–	**−1.76E +00**	2.59E-05	*−1.95E-04*
Insula L	571.52	6582.2	**−8.16E +00**	6.57E-02	–	*5.74E+01*	**3.15E-03**	**1.41E-09**	–	**−7.18E +01**	**−1.37E +02**	**−1.40E +02**	–	–	2.07E-04	**−3.34E +00**	–	–
Insula R	629.95	6724.1	**−6.75E +00**	–	–	**1.10E +02**	**3.30E-03**	**1.47E-09**	–	**−1.70E +02**	**−2.09E +02**	**−3.28E +02**	*1.74E+02*	**3.92E +02**	2.81E-04	*−2.34E +00*	**6.29E-04**	−1.55E-04
Cortex L	13274.07	226477.6	**−4.98E +02**	**4.28E +00**	**−2.45E-01**	**1.26E +03**	1.14E-01	2.97E-08	**−5.93E-14**	**−7.50E +03**	**2.15E+03**	−9.66E+03	**−7.52E +03**	5.64E+03	–	−8.95E +01	6.48E-03	−9.45E-03
Cortex R	13261.90	227468.1	**−4.89E +02**	**3.98E +00**	**−2.34E-01**	*1.71E+03*	**1.12E-01**	**3.18E-08**	−3.96E-14	**−7.40E +03**	**8.21E+02**	−9.01E+03	**−7.54E +03**	4.91E+03	–	−9.73E +01	**7.19E-04**	−1.35E-02

Note. Categories are coded 0 and 1 with reference categories (Female, Siemens, and 3T) coded 0. Age and eTIV are centered by the mean (Age – 47.58; eTIV – 1528926.15). Int: Intercept. RMSE: Root mean square error. STS: Superior temporal sulcus.

Italic $p < .05$; **Bold** $p < .01$.

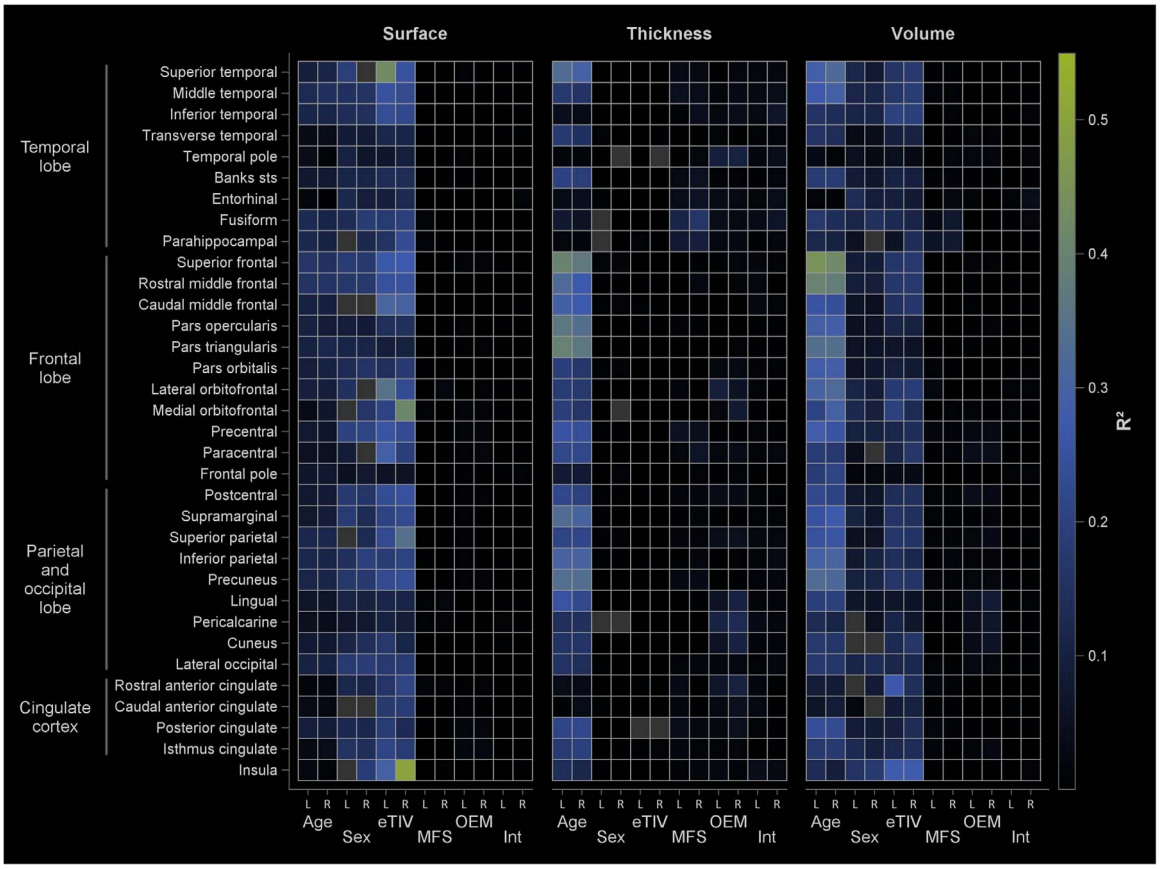

Fig. 4. R^2 maps for each predictor according to regional cortical surface area, thickness, and volume. Gray rectangles denote predictors not retained in the models. eTIV: estimated intracranial volume. MFS: Magnetic field strength. OEM: Original equipment manufacturer. Int: Interactions.

small impact on the surface, thickness, and volume of the whole cortex. Adding these two variables to the final models yielded a mean R^2 increased of 2.5% (range between 1.2–4.2). Therefore, we chose not to include these variables into the predictive models.

Influence of computer hardware setups

The influence of computer hardware setups to generate *FreeSurfer* surface areas, thicknesses, and volumes was minor. The mean of all regional mean absolute differences was below 0.4% in surface area (0.39%, SD: 0.39%), thickness (0.21%, 0.19%) and volume (0.36%, 0.42%) and no significant difference between setups was observed (Supplemental Table 2).

Discussion

Normative data are highly valuable in health sciences and are commonly used in a number of fields (e.g. neuropsychology). Neuroimaging lags in this respect, as normative values are nearly nonexistent. The present study is an attempt to continue to fill this methodological gap by developing normative data for regional cortical surface areas, thicknesses, and volumes in healthy adults according to age, sex, eTIV, and scanner MFS and manufacturer. The results clearly show that age, sex, and eTIV have major influences on these cortical measures and need to be taken into account to assess deviations from the mean of healthy adults. The models predicting normative values were validated in an independent sample of healthy adults and analyses in individuals with SZ and mild AD confirmed the ability of the normative values to detect morphometric normality deviations.

Use of the normative data.

In order to properly use the normative data, the user must produce morphometric measures with *FreeSurfer* 5.3 with default parameters, that is, “recon-all -all” without any flag option. Within the manuscript we provide formulas in order to compute expected surface areas, thicknesses, and volumes according to an individual's characteristics alongside those of the scanner being used, as well as Z scores indicating the effect size of the deviation from the normative sample. We have included as Supplementary materials a Microsoft Excel spreadsheet able to compute Z scores for an individual, as well as various statistics including single case significance test of volume abnormality and estimated percentage of the normative population with a smaller volume. In addition, we provide a python script producing normative Z scores for multiple participants using the default cortical atlas (Desikan-Killiany), but also able to use other parcellation protocols including Desikan-Killiany-Tourville, Ex vivo (Potvin et al., 2017) and subcortical atlases (Potvin et al., 2016b).

For example, using formulas for the whole left cortical hemisphere, a 66 year old female with an eTIV of 1528670 mm^3 (estimation from *FreeSurfer*) scanned on a Siemens 3T would be expected to have a surface area of 81389 mm^2, a thickness of 2.40 mm, and a volume of 217210 mm^3. In the event that the measured left cortex of this individual has a surface area of 80100 mm^2, a thickness of 2.20 mm, and a volume of 193589 mm^3, the difference between the real value (Observed) and the expected normative value (Predicted) divided by the root mean square of the predicting models yield effect size Z scores (Z_{OP}) of −0.28, −1.98, and −1.78, respectively. These Z scores, which have a mean of 0 and a standard deviation (SD) of 1, indicate that compared to the normative sample, this person has a thickness and volume of nearly 2 SDs below what is expected for her age, sex, and eTIV.

Z_{OP} effect size can be useful in assessing the deviation from the normality of an individual, but also of groups, as illustrated in Figs. 9

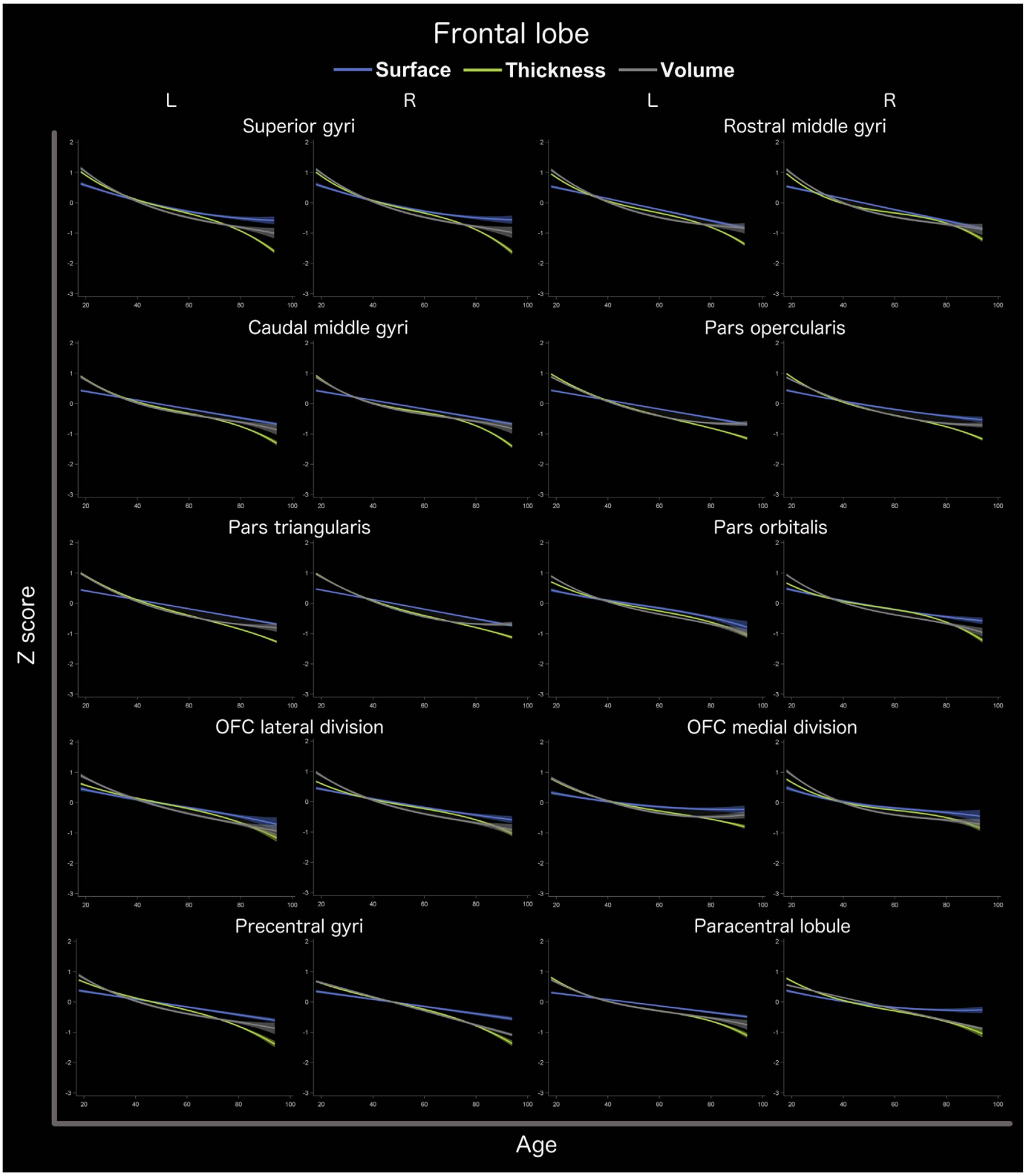

Fig. 5. Standardized predicted surface area, thickness, and volume of frontal lobe regions according to age derived from the models built to produce the normative values. Shaded ribbons around each curve denote 95% confidence intervals for the mean. L: Left. R: Right.

and 10. Individuals with SZ and mild AD showed Z_{OP} score deviations in regional cortical measures that were expected (Bakkour et al., 2009; Dickerson et al., 2009; Haijma et al., 2013; Sabuncu et al., 2011; Vita et al., 2012). For SZ, deviations from the normative sample were observed in several regions with the highest effect sizes being mainly in frontal and lateral temporal areas. For mild AD, deviations from the normative sample were also noticed in many regions, but were especially prominent for the medial temporal, temporopolar and lateral temporal cortices, and inferior parietal cortex. Z_{OP} effect size can also be particularly valuable for case-control study in order to evaluate how well the morphometric measures of a control group compare with the normative values. Indeed, small control groups are unlikely to be

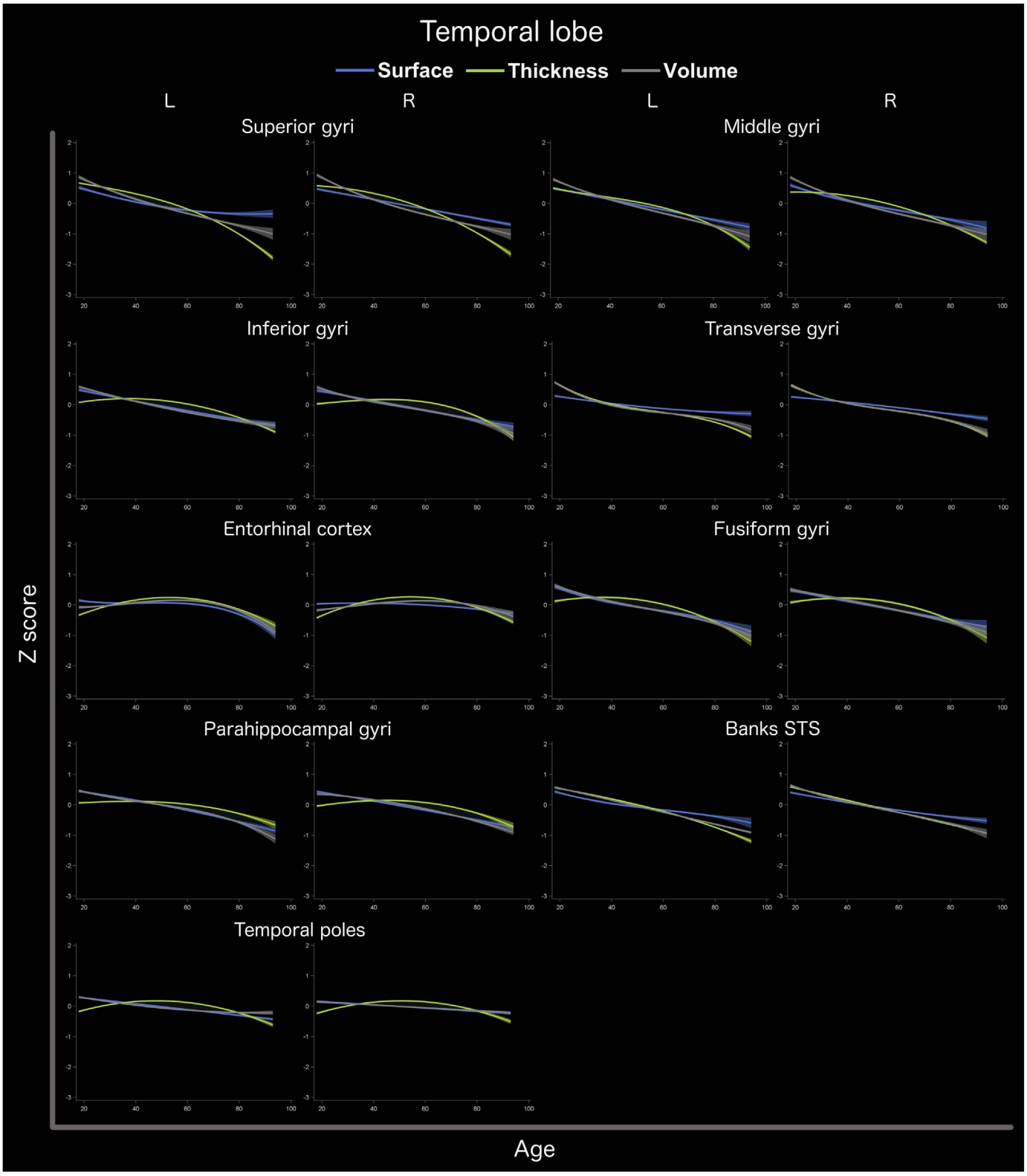

Fig. 6. Standardized predicted surface area, thickness, and volume of temporal lobe regions according to age derived from the models built to produce the normative values. Shaded ribbons around each curve denote 95% confidence intervals for the mean. L: Left. R: Right.

representative of the healthy adult population and it might result in overestimating or underestimating case-control differences.

One should note that model fit strongly varies according to brain regions and measures. Therefore, the higher the model R^2 is, the more sensitive the normative Z score or Z_{OP} is likely to detect normality deviation compared to the raw value (surface area/thickness/volume) because its denominator (RMSE) will be smaller. Conversely, models with low R^2 will likely result in abnormality detection closer to what would be obtained using raw values since their denominator are high.

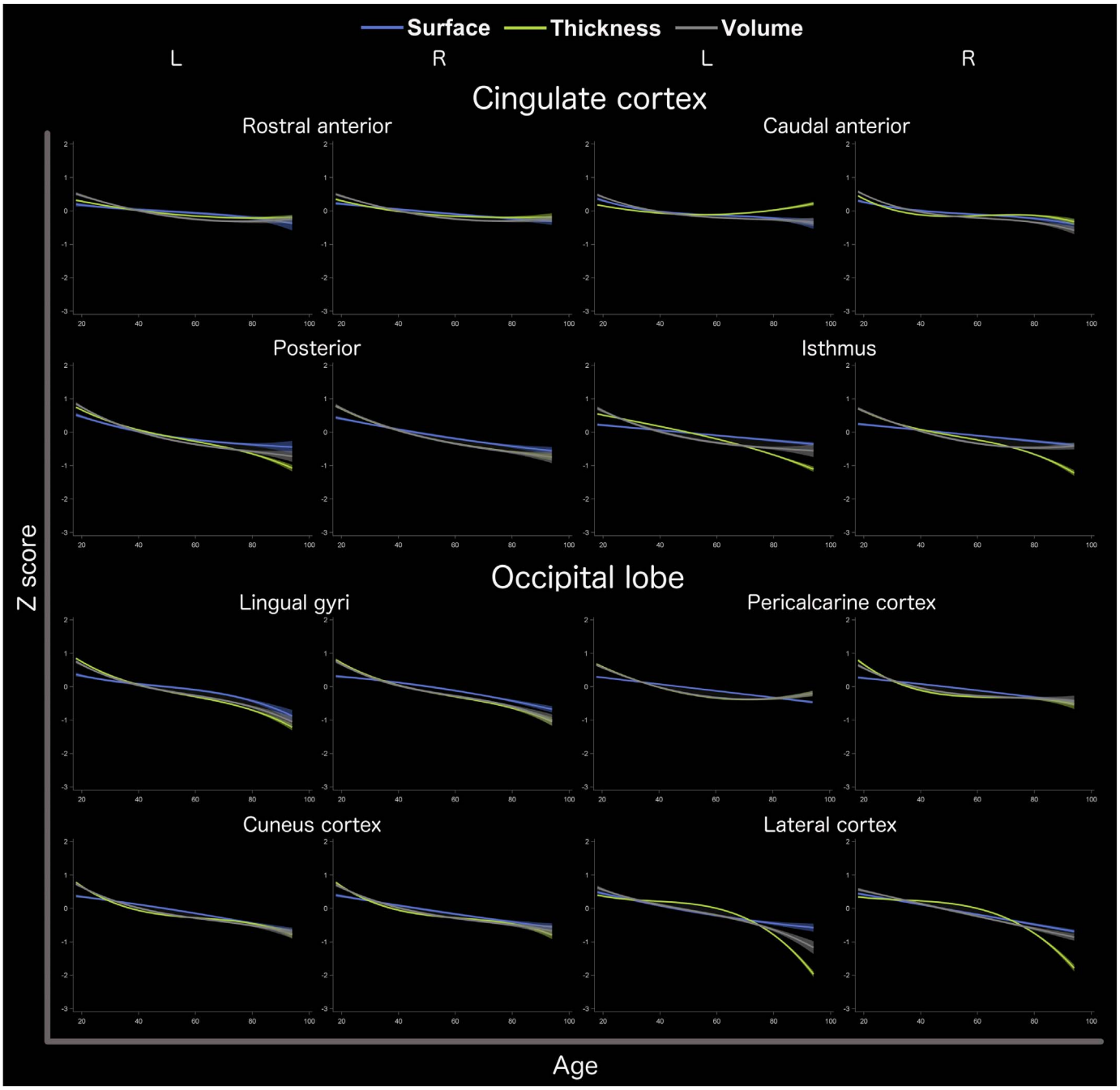

Fig. 7. Standardized predicted surface area, thickness, and volume of cingulate and occipital regions according to age derived from the models built to produce the normative values. Shaded ribbons around each curve denote 95% confidence intervals for the mean. L: Left. R: Right.

Effect of age

Despite the fact that the predictors selection procedure retained quadratic and cubic age terms for better predictions in most regions, age plots show that age effects for surface area and volume were essentially linear, but for thickness, the measure generally appears to decrease at a higher rate when age was above 60 years old. Our results seem similar to that of other groups (McKay et al., 2014; Storsve et al., 2014). For example, the non-linear relationships of age on thickness replicate results from McKay et al. with a sizable (N=1010) sample (McKay et al., 2014), which showed quadratic effects in most cortical regions for thickness, but not for surface area. Moreover, unlike most regions, the thickness of the entorhinal cortex and temporal pole were nearly flat or slightly increased until the fifth decade of life before slightly declining. Similar results were also observed in another study using a large (N=1660) sample (Hasan et al., 2016), but other results from adults of similar age (23–87 years old) showed a relatively stable thickness before declining after the sixth decade of life (Storsve et al., 2014). Indeed, the impact of age on the thickness of the entorhinal cortex and temporal pole was minimal ($R^2 < 5\%$) unlike nearly all other regions in our study. This makes sense with results from a twin study suggesting that the entorhinal cortex was one of the regions that was most highly influenced by environmental factors in terms of surface area and thickness (Panizzon et al., 2009).

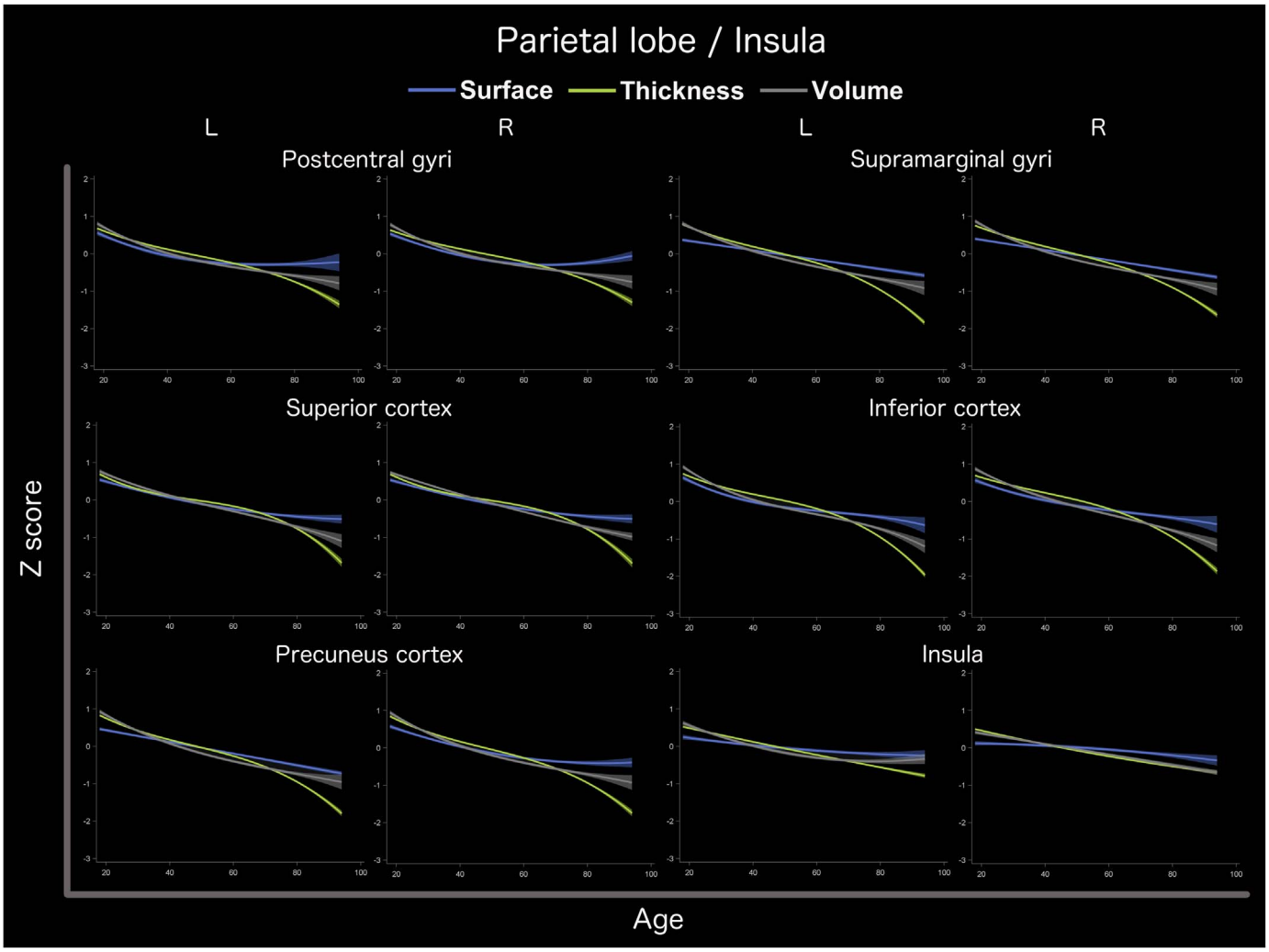

Fig. 8. Standardized predicted surface area, thickness, and volume of parietal lobe regions and insula according to age derived from the models built to produce the normative values. Shaded ribbons around each curve denote 95% confidence intervals for the mean. L: Left. R: Right.

Differences between men and women

Many studies using various methodologies attempted to measure differences between men and women in terms of cortical volume (Fjell et al., 2009; Jancke et al., 2015; Pfefferbaum et al., 2013; Pintzka et al., 2015; Sowell et al., 2007) and thickness (Fjell et al., 2009; Govindarajan et al., 2014; Luders et al., 2006; McKay et al., 2014; Sowell et al., 2007), generally focusing on the whole cortex. For cortical volume, the conclusions of these studies were that the effect of sex disappeared or was minor (with men having larger cortical volumes) when taking into account head compartment volume. For example, one study using a large sample reported that men had significant larger cerebral cortex volumes than women after removing the variance explained by eTIV with a difference in terms of standardized residuals of approximately 0.2 (Fjell et al., 2009). For cortical thickness, the conclusions are inconsistent between studies. Fjell et al. (2009), as well as others (Govindarajan et al., 2014; McKay et al., 2014), reported no significant cortical thickness differences between men and women, but other results in well matched young adults indicated thicker cortex in women compared to men in most cortical areas (Luders et al., 2006) while another study using a wide age range (7 to 87 years old) observed the same effect, but specifically in the inferior parietal, lateral temporal, and inferior frontal regions (Sowell et al., 2007). However, these discrepancies are likely to be related to differences in segmentation techniques since the former studies (Fjell et al., 2009; Govindarajan et al., 2014; McKay et al., 2014) used *FreeSurfer* while the latter studies (Luders et al., 2006; Sowell et al., 2007) used in-house algorithms.

Unlike these previous studies, our approach allowed for a systematic comparison of the respective weight (R^2) of each predictors' effect on cortical morphometric measures. Our results on whole hemispheres indicated that sex had a greater effect on cortical surface area than age, nearly no effect on cortical thickness, and a smaller, but substantial, effect on cortical volume compared to age and eTIV. Despite methodological differences, this corroborates to some extent previous findings showing that compared to women, men have somewhat larger cortical volumes (Fjell et al., 2009) due to differences in terms of cortical surface area (McKay et al., 2014) rather than cortical thickness. Furthermore, in terms of regional measures, our models showed that men had generally larger regional surface areas and volumes than women, but women had thicker cortex compared to men in most areas. However, the magnitude of the sex effects for cortical thickness were negligible ($R^2 < 2\%$), in line with previous studies who reported minimal or no sex effect on cortical thickness (Fjell et al., 2009; McKay et al., 2014).

In line with previous reports using large samples, we did not observe substantial age by sex interactions ($R^2 < 1\%$), indicating that the morphometric changes through aging is equivalent between men and women (Fjell et al., 2009; Pfefferbaum et al., 2013; Sowell et al., 2007; see also Thambisetty et al., 2010).

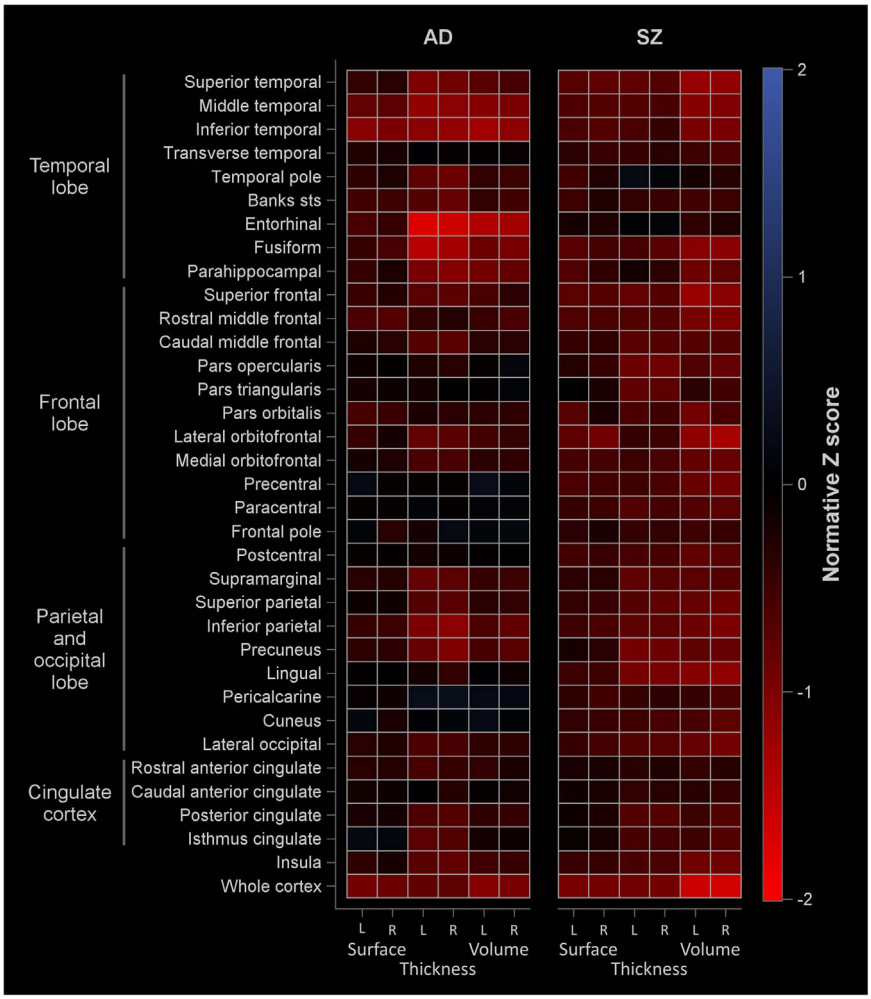

Fig. 9. Z_{OP} effect size maps for each mean regional cortical surface area, thickness, and volume in individuals with schizophrenia (SZ) and individuals with mild Alzheimer's disease (AD).

Magnetic field strength and scanner manufacturer

Similar to our previous results on subcortical regions (Potvin et al., 2016b), MFS and manufacturer had limited effects on cortical measures compared to age, sex and eTIV. The influence of these factors on surface areas and volumes was generally minimal, but was more important for thickness, which could be substantially influenced by MFS depending on the region (R^2 range 0 to 16%). Our results agree with previous reports (Govindarajan et al., 2014) which state that 1.5T MFS generally yields thinner cortex than 3T for most areas, but with some exceptions (e.g. cuneus, pericalcarine, frontal poles), with increased thickness at 1.5T compared to 3T. The influence of MFS is not surprising since cortical thickness relies on identification of white matter and pial surface areas and higher MFS results in better white/gray matter contrast (Kruggel et al., 2010), which in turn is likely to improve accuracy of detecting these boundaries.

Limitations

The sample used in the present study was recruited using a non-probability sampling method and is therefore not necessarily representative of the healthy adult-population. In fact, it included healthy participants that volunteered for research studies involving MRI in academic-led environments. Based on the available characteristics, the participants were mainly right-handed Caucasians with at least a high school degree. Nevertheless, the sample was one of the largest used in such studies (nearly 3000 participants), encompassing 23 subsamples provided by 21 independent research groups, including participants from various countries (Australia, Austria, Belgium, Canada, Finland, Germany, Ireland, Italy, Netherlands, United Kingdom, and USA), as well as images originating from three scanner manufacturers at either 1.5T or 3T. Such an amalgam of data is likely to be more representative and yield more robust normative values than results produced within restricted geographical regions and using specific scanner characteristics. Indeed, our validation procedure using a randomly selected, independent sample showed highly concordant predictions in terms of R^2 for nearly all measures.

Due to its relatively recent development and use in medicine over the last two decades, longitudinal MRIs of individuals throughout their lifetimes are not available at the moment. The design of our study was cross-sectional and thus, may encompass cohort biases. For example, we cannot rule out differences of brain developments between older and younger participants due to specific environmental differences (e.g. diet, education and medical care access). However, further studies using longitudinal scans over several years might help controlling to some extent potential cohort biases. Moreover, while we included two central scanner characteristics (i.e. MFS and manufacturer), it was not possible to take into account the potential influence of many others. For example, scan sequence, scanner model within manufacturers, and coil type, can have an impact on derived morphometric measures (Kruggel et al., 2010). Finally, many morphometric measures had non-linear age effects and future work are needed to verify whether norms solely based on older adults would be more sensitive to normality deviation in this population than norms based on a wider age range such as the present study.

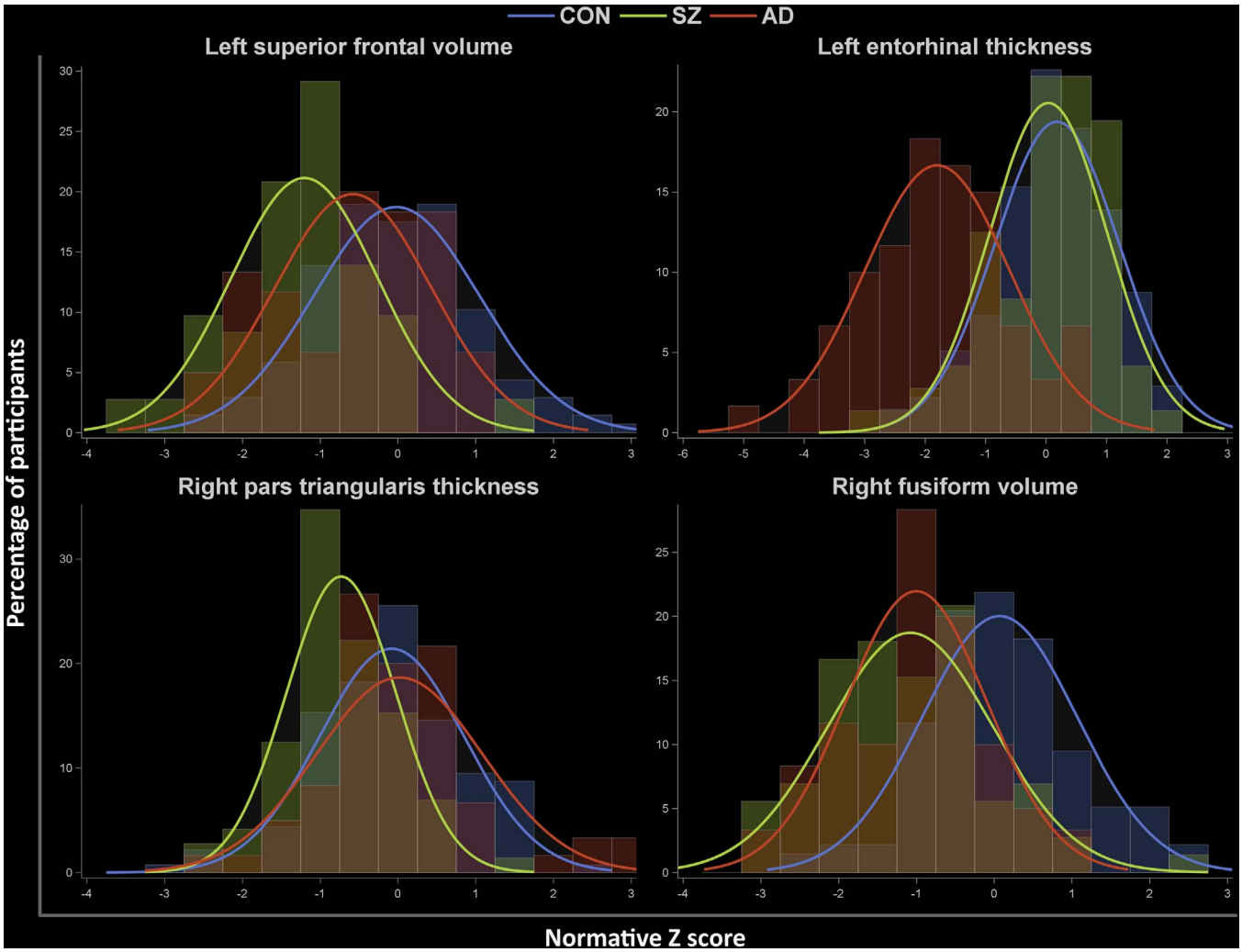

Fig. 10. Examples of distributions of the normative effect sizes (Z_{OP} score) in independent samples of healthy controls (CON), individuals with schizophrenia (SZ), and individuals with mild Alzheimer's disease (AD).

Conclusions

The present study is the first attempt to produce normative values for morphometric cortical measures. Normative values based on an individual's and scanner's characteristics are essential to adequately assess deviations from normality. The generated values are meant to be reused by other neuroimaging research groups, via the Supplementary material provided, which easily compute estimates of expected surface area, thickness and volume, as well as Z score effect sizes denoting the extent of the deviation from the normative sample, single case significance test of value abnormality, and estimated percentage of the normative population with a smaller surface area, thickness or volume.

Conflict of interest

O.P. and L.D. declare no competing financial interests. S.D. is officer and shareholder of True Positive Medical Devices inc.

Acknowledgments

We gratefully acknowledge financial support from the Alzheimer's Society of Canada (#13–32), the Canadian Foundation for Innovation (#30469), the Fonds de recherche du Québec – Santé / Pfizer Canada - Pfizer-FRQS Innovation Fund (#25262), and the Canadian Institute for Health Research (#117121). S.D. is a Research Scholar from the Fonds de recherche du Québec – Santé (#30801).

This study comprises multiple samples of healthy individuals. We wish to thank all principal investigators who collected these datasets and agreed to let them accessible.

Autism Brain Imaging Data Exchange (ABIDE): Primary support for the work by Adriana Di Martino was provided by the NIMH (K23MH087770) and the Leon Levy Foundation. Primary support for the work by Michael P. Milham and the INDI team was provided by gifts from Joseph P. Healy and the Stavros Niarchos Foundation to the Child Mind Institute, as well as by an NIMH award to MPM (R03MH096321). http://fcon_1000.projects.nitrc.org/indi/abide/.

Alzheimer's Disease Neuroimaging Initiative (ADNI): Funded by the ADNI (National Institutes of Health Grant U01 AG024904) and DOD ADNI (Department of Defense award number W81XWH-12-2-0012). ADNI is funded by the National Institute on Aging, the National Institute of Biomedical Imaging and Bioengineering, and through generous contributions from the following: AbbVie, Alzheimer's Association; Alzheimer's Drug Discovery Foundation; Araclon Biotech; BioClinica, Inc.; Biogen; Bristol-Myers Squibb Company; CereSpir, Inc.; Eisai Inc.; Elan Pharmaceuticals, Inc.; Eli Lilly and Company; EuroImmun; F. Hoffmann-La Roche Ltd and its affiliated company Genentech, Inc.; Fujirebio; GE Healthcare; IXICO Ltd.; Janssen Alzheimer Immunotherapy Research & Development, LLC.; Johnson & Johnson Pharmaceutical Research & Development LLC.;

Lumosity; Lundbeck; Merck & Co., Inc.; Meso Scale Diagnostics, LLC.; NeuroRx Research; Neurotrack Technologies; Novartis Pharmaceuticals Corporation; Pfizer Inc.; Piramal Imaging; Servier; Takeda Pharmaceutical Company; and Transition Therapeutics. The Canadian Institutes of Health Research is providing funds to support ADNI clinical sites in Canada. Private sector contributions are facilitated by the Foundation for the National Institutes of Health (www.fnih.org). The grantee organization is the Northern California Institute for Research and Education, and the study is coordinated by the Alzheimer's Disease Cooperative Study at the University of California, San Diego. ADNI data are disseminated by the Laboratory for Neuro Imaging at the University of Southern California. http://adni.loni.usc.edu/.

Australian Imaging Biomarkers and Lifestyle flagship study of ageing (AIBL): Part of the data used in this study was obtained from the Australian Imaging Biomarkers and Lifestyle flagship study of ageing (AIBL) funded by the Commonwealth Scientific and Industrial Research Organisation (CSIRO) which was made available at the ADNI database (www.loni.usc.edu/ADNI). The AIBL researchers contributed data but did not participate in analysis or writing of this report. AIBL researchers are listed at www.aibl.csiro.au.

BMB - Berlin Mind and Brain (Margulies, Villringer). Zuo et al. (2014). An open science resource for establishing reliability and reproducibility in functional connectomics. *Scientific data, 1*, 140049. doi: 10.1038/sdata.2014.49. http://fcon_1000.projects.nitrc.org/indi/CoRR/html/bmb_1.html.

Cleveland Clinic (Cleveland CCF): Funded by the National Multiple Sclerosis Society. http://fcon_1000.projects.nitrc.org/indi/retro/ClevelandCCF.html.

Center of Biomedical Research Excellence (COBRE): The imaging data and phenotypic information was collected and shared by the Mind Research Network and the University of New Mexico funded by a National Institute of Health COBRE: 1P20RR021938-01A2. http://fcon_1000.projects.nitrc.org/indi/retro/cobre.html.

DS-108. Wager et al. (2008). Prefrontal-subcortical pathways mediating successful emotion regulation. Neuron, 59(6):1037-50. doi: 10.1016/j.neuron.2008.09.006. This data was obtained from the OpenfMRI database. NSF Grant OCI-1131441 (R. Poldrack, PI). Poldrack et al. (2013). Toward open sharing of task-based fMRI data: the OpenfMRI project. *Frontiers in neuroinformatics, 7*, 12. doi: 10.3389/fninf.2013.00012. https://openfmri.org/dataset/ds000108/.

DS-170. Learning and memory: motor skill consolidation and intermanual transfer. This data was obtained from the OpenfMRI database. NSF Grant OCI-1131441 (R. Poldrack, PI). Poldrack et al. (2013). Toward open sharing of task-based fMRI data: the OpenfMRI project. *Frontiers in neuroinformatics, 7*, 12. doi: 10.3389/fninf.2013.00012. https://openfmri.org/dataset/ds000170/.

Functional Biomedical Informatics Research Network (FBIRN): Provided by the Biomedical Informatics Research Network under the following support: U24-RR021992, by the National Center for Research Resources at the National Institutes of Health, U.S.A. http://www.birncommunity.org/resources/data/.

FIND lab sample. Funded by the Dana Foundation; John Douglas French Alzheimer's Foundation; National Institutes of Health (AT005733, HD059205,HD057610, NS073498, NS058899).

http://fcon_1000.projects.nitrc.org/indi/retro/find_stanford.html.

International Consortium for Brain Mapping (ICBM). http://www.loni.usc.edu/ICBM/.

Information eXtraction from Images (IXI): Data collected as part of the project:

EPSRC GR/S21533/02 - http://www.brain-development.org/.

F.M. Kirby Research Center neuroimaging reproducibility data (KIRBY-21). Landman, B.A. et al. “Multi-Parametric Neuroimaging Reproducibility: A 3T Resource Study”, NeuroImage. (2010) NIHMS/PMC:252138 doi:10.1016/j.neuroimage.2010.11.047 http://mri.kennedykrieger.org/databases.html.

Minimal Interval Resonance Imaging in Alzheimer's Disease (MIRIAD): The MIRIAD investigators did not participate in analysis or writing of this report. The MIRIAD dataset is made available through the support of the UK Alzheimer's Society (RF116). The original data collection was funded through an unrestricted educational grant from GlaxoSmithKline (6GKC). http://miriad.drc.ion.ucl.ac.uk.

Nathan Kline Institute Rockland (NKI-R) sample (phase 1) and (phase 2): Principal support for the enhanced NKI-RS project is provided by the NIMH BRAINS R01MH094639-01. Funding for key personnel also provided in part by the New York State Office of Mental Health and Research Foundation for Mental Hygiene. Funding for the decompression and augmentation of administrative and phenotypic protocols provided by a grant from the Child Mind Institute (1FDN2012-1). Additional personnel support provided by the Center for the Developing Brain at the Child Mind Institute, as well as NIMH R01MH081218, R01MH083246, and R21MH084126. Project support also provided by the NKI Center for Advanced Brain Imaging (CABI), the Brain Research Foundation, the Stavros Niarchos Foundation and the NIH P50 MH086385-S1 (phase 1). http://fcon_1000.projects.nitrc.org/indi/pro/nki.html http://fcon_1000.projects.nitrc.org/indi/enhanced/.

Open access series of imaging studies (OASIS): The OASIS project was funded by grants P50 AG05681, P01 AG03991, R01 AG021910, P50 MH071616, U24 RR021382, and R01 MH56584. http://www.oasis-brains.org/.

POWER: This database was supported by NIH R21NS061144 R01NS32979 R01HD057076 U54MH091657 K23DC006638 P50 MH71616 P60 DK020579-31, McDonnell Foundation Collaborative Action Award, NSF IGERT DGE-0548890, Simon's Foundation Autism Research Initiative grant, Burroughs Wellcome Fund, Charles A. Dana Foundation, Brooks Family Fund, Tourette Syndrome Association, Barnes-Jewish Hospital Foundation, McDonnell Center for Systems Neuroscience, Alvin J. Siteman Cancer Center, American Hearing Research Foundation grant, Diabetes Research and Training Center at Washington University grant. http://fcon_1000.projects.nitrc.org/indi/retro/Power2012.html.

Parkinson's Progression Markers Initiative (PPMI): PPMI – a public-private partnership – is funded by the Michael J. Fox Foundation for Parkinson's Research and funding partners, including Abbvie, Avid Radiopharmaceuticals, Biogen Idec, Bristol-Myers, Covance, GE Healthcare, Genentech, GlaxoSmithKline, Eli Lilly and Company, Lundbeck, Merck, Meso Scale Discovery, Pfizer, Piramal, Roche, and UCB. See http://www.ppmi-info.org for further details.

TRAIN-39: Data collected at the Biomedical Imaging Center at the Beckman Institute for Advanced Science and Technology at UIUC. Funded by the Office of Naval Research (ONR): N00014-07-1–0903. http://fcon_1000.projects.nitrc.org/indi/retro/Train-39.html.

University of Wisconsin, Madison (Birn, Prabhakaran, Meyerand) CoRR sample (UWM). Zuo et al. (2014). An open science resource for establishing reliability and reproducibility in functional connectomics. *Scientific data, 1*, 140049. doi: 10.1038/sdata.2014.49.

http://fcon_1000.projects.nitrc.org/indi/CoRR/html/samples.html.

Appendix A. Supplementary material

Supplementary data associated with this article can be found in the online version at doi:10.1016/j.neuroimage.2017.05.019.

References

Bakkour, A., Morris, J.C., Dickerson, B.C., 2009. The cortical signature of prodromal AD: regional thinning predicts mild AD dementia. Neurology 72, 1048–1055.

Barnes, J., Ridgway, G.R., Bartlett, J., Henley, S.M., Lehmann, M., Hobbs, N., Clarkson, M.J., MacManus, D.G., Ourselin, S., Fox, N.C., 2010. Head size, age and gender adjustment in MRI studies: a necessary nuisance? Neuroimage 53, 1244–1255.

Buckner, R.L., Head, D., Parker, J., Fotenos, A.F., Marcus, D., Morris, J.C., Snyder, A.Z.,

2004. A unified approach for morphometric and functional data analysis in young, old, and demented adults using automated atlas-based head size normalization: reliability and validation against manual measurement of total intracranial volume. Neuroimage 23, 724–738.
Crawford, J.R., Garthwaite, P.H., 2006. Comparing patients' predicted test scores from a regression equation with their obtained scores: a significance test and point estimate of abnormality with accompanying confidence limits. Neuropsychology 20, 259–271.
Crawford, J.R., Garthwaite, P.H., Denham, A.K., Chelune, G.J., 2012. Using regression equations built from summary data in the psychological assessment of the individual case: extension to multiple regression. Psychol. Assess. 24, 801–814.
Crivello, F., Tzourio-Mazoyer, N., Tzourio, C., Mazoyer, B., 2014. Longitudinal assessment of global and regional rate of grey matter atrophy in 1,172 healthy older adults: modulation by sex and age. PLoS One 9, e114478.
Dale, A.M., Fischl, B., Sereno, M.I., 1999. Cortical surface-based analysis. I. Segmentation and surface reconstruction. Neuroimage 9, 179–194.
Dale, A.M., Sereno, M.I., 1993. Improved Localizadon of cortical activity by combining EEG and MEG with MRI cortical surface reconstruction: a linear approach. J Cogn. Neurosci. 5, 162–176.
Desikan, R.S., Segonne, F., Fischl, B., Quinn, B.T., Dickerson, B.C., Blacker, D., Buckner, R.L., Dale, A.M., Maguire, R.P., Hyman, B.T., Albert, M.S., Killiany, R.J., 2006. An automated labeling system for subdividing the human cerebral cortex on MRI scans into gyral based regions of interest. Neuroimage 31, 968–980.
Dickerson, B.C., Bakkour, A., Salat, D.H., Feczko, E., Pacheco, J., Greve, D.N., Grodstein, F., Wright, C.I., Blacker, D., Rosas, H.D., Sperling, R.A., Atri, A., Growdon, J.H., Hyman, B.T., Morris, J.C., Fischl, B., Buckner, R.L., 2009. The cortical signature of Alzheimer's disease: regionally specific cortical thinning relates to symptom severity in very mild to mild AD dementia and is detectable in asymptomatic amyloid-positive individuals. Cereb. Cortex 19, 497–510.
Ellis, K.A., Bush, A.I., Darby, D., De Fazio, D., Foster, J., Hudson, P., Lautenschlager, N.T., Lenzo, N., Martins, R.N., Maruff, P., Masters, C., Milner, A., Pike, K., Rowe, C., Savage, G., Szoeke, C., Taddei, K., Villemagne, V., Woodward, M., Ames, D., Group, A.R., 2009. The Australian Imaging, Biomarkers and Lifestyle (AIBL) study of aging: methodology and baseline characteristics of 1112 individuals recruited for a longitudinal study of Alzheimer's disease. Int. psychogeriatrics/IPA 21, 672–687.
First, M.B., Spitzer, R.L., Gibbon, M., Williams, J.B.W., 1996. Structured Clinical Interview for DSM-IV Axis I Disorders (SCID), clinician version. American Psychiatric Press, Washington D.C.
Fischl, B., 2012. FreeSurfer. Neuroimage 62, 774–781.
Fischl, B., Dale, A.M., 2000. Measuring the thickness of the human cerebral cortex from magnetic resonance images. Proc. Natl. Acad. Sci. USA 97, 11050–11055.
Fischl, B., Liu, A., Dale, A.M., 2001. Automated manifold surgery: constructing geometrically accurate and topologically correct models of the human cerebral cortex. IEEE Trans. Medi Imaging 20, 70–80.
Fischl, B., Sereno, M.I., Dale, A.M., 1999a. Cortical surface-based analysis. II: inflation, flattening, and a surface-based coordinate system. Neuroimage 9, 195–207.
Fischl, B., Sereno, M.I., Tootell, R.B., Dale, A.M., 1999b. High-resolution intersubject averaging and a coordinate system for the cortical surface. Hum. Brain Mapp. 8, 272–284.
Fischl, B., van der Kouwe, A., Destrieux, C., Halgren, E., Segonne, F., Salat, D.H., Busa, E., Seidman, L.J., Goldstein, J., Kennedy, D., Caviness, V., Makris, N., Rosen, B., Dale, A.M., 2004. Automatically parcellating the human cerebral cortex. Cereb. Cortex 14, 11–22.
Fjell, A.M., Westlye, L.T., Amlien, I., Espeseth, T., Reinvang, I., Raz, N., Agartz, I., Salat, D.H., Greve, D.N., Fischl, B., Dale, A.M., Walhovd, K.B., 2009. Minute effects of sex on the aging brain: a multisample magnetic resonance imaging study of healthy aging and Alzheimer's disease. J. Neurosci. 29, 8774–8783.
Govindarajan, K.A., Freeman, L., Cai, C., Rahbar, M.H., Narayana, P.A., 2014. Effect of intrinsic and extrinsic factors on global and regional cortical thickness. PLoS One 9, e96429.
Haijma, S.V., Van Haren, N., Cahn, W., Koolschijn, P.C., Hulshoff Pol, H.E., Kahn, R.S., 2013. Brain volumes in schizophrenia: a meta-analysis in over 18 000 subjects. Schizophr. Bull. 39, 1129–1138.
Han, X., Jovicich, J., Salat, D., van der Kouwe, A., Quinn, B., Czanner, S., Busa, E., Pacheco, J., Albert, M., Killiany, R., Maguire, P., Rosas, D., Makris, N., Dale, A., Dickerson, B., Fischl, B., 2006. Reliability of MRI-derived measurements of human cerebral cortical thickness: the effects of field strength, scanner upgrade and manufacturer. Neuroimage 32, 180–194.
Hasan, K.M., Mwangi, B., Cao, B., Keser, Z., Tustison, N.J., Kochunov, P., Frye, R.E., Savatic, M., Soares, J., 2016. Entorhinal Cortex Thickness across the Human Lifespan. J Neuroimaging 26, 278–282.
Hastie, T., Tibshirani, R., Friedman, J., 2008. The elements of statistical learning. Data mining, inference, and prediction. Springer.
Jancke, L., Merillat, S., Liem, F., Hanggi, J., 2015. Brain size, sex, and the aging brain. Hum. Brain Mapp. 36, 150–169.
Kruggel, F., 2006. MRI-based volumetry of head compartments: normative values of healthy adults. Neuroimage 30, 1–11.
Kruggel, F., Turner, J., Muftuler, L.T., 2010. Impact of scanner hardware and imaging protocol on image quality and compartment volume precision in the ADNI cohort. Neuroimage 49, 2123–2133.
Kuperberg, G.R., Broome, M.R., McGuire, P.K., David, A.S., Eddy, M., Ozawa, F., Goff, D., West, W.C., Williams, S.C., van der Kouwe, A.J., Salat, D.H., Dale, A.M., Fischl, B., 2003. Regionally localized thinning of the cerebral cortex in schizophrenia. Arch. Gen. Psychiatry 60, 878–888.
Luders, E., Narr, K.L., Thompson, P.M., Rex, D.E., Woods, R.P., Deluca, H., Jancke, L., Toga, A.W., 2006. Gender effects on cortical thickness and the influence of scaling. Hum. Brain Mapp. 27, 314–324.
McKay, D.R., Knowles, E.E., Winkler, A.A., Sprooten, E., Kochunov, P., Olvera, R.L., Curran, J.E., Kent, J.W., Jr., Carless, M.A., Goring, H.H., Dyer, T.D., Duggirala, R., Almasy, L., Fox, P.T., Blangero, J., Glahn, D.C., 2014. Influence of age, sex and genetic factors on the human brain. Brain Imaging Behav. 8, 143–152.
McKhann, G., Drachman, D., Folstein, M., Katzman, R., Price, D., Stadlan, E.M., 1984. Clinical diagnosis of Alzheimer's disease: report of the NINCDS-ADRDA work group under the auspices of Department of Health and Human Services Task Force on Alzheimer's Disease. Neurology 34, 939–944.
Panizzon, M.S., Fennema-Notestine, C., Eyler, L.T., Jernigan, T.L., Prom-Wormley, E., Neale, M., Jacobson, K., Lyons, M.J., Grant, M.D., Franz, C.E., Xian, H., Tsuang, M., Fischl, B., Seidman, L., Dale, A., Kremen, W.S., 2009. Distinct genetic influences on cortical surface area and cortical thickness. Cereb. Cortex 19, 2728–2735.
Pfefferbaum, A., Rohlfing, T., Rosenbloom, M.J., Chu, W., Colrain, I.M., Sullivan, E.V., 2013. Variation in longitudinal trajectories of regional brain volumes of healthy men and women (ages 10 to 85 years) measured with atlas-based parcellation of MRI. Neuroimage 65, 176–193.
Pintzka, C.W., Hansen, T.I., Evensmoen, H.R., Haberg, A.K., 2015. Marked effects of intracranial volume correction methods on sex differences in neuroanatomical structures: a HUNT MRI study. Front. Neurosci. 9, 238.
Potvin, O., Dieumegarde, L., Duchesne, S., 2017. Freesurfer cortical normative data for adults using Desikan-Killiany-Tourville and ex vivo protocols. Neuroimage 156, 43–64.
Potvin, O., Mouiha, A., Dieumegarde, L., Duchesne, S., 2016a. FreeSurfer subcortical normative data. Data Brief 9, 732–736.
Potvin, O., Mouiha, A., Dieumegarde, L., Duchesne, S., 2016b. Normative data for subcortical regional volumes over the lifetime of the adult human brain. Neuroimage 137, 9–20.
Reuter, M., Rosas, H.D., Fischl, B., 2010. Highly accurate inverse consistent registration: a robust approach. Neuroimage 53, 1181–1196.
Rosas, H.D., Liu, A.K., Hersch, S., Glessner, M., Ferrante, R.J., Salat, D.H., van der Kouwe, A., Jenkins, B.G., Dale, A.M., Fischl, B., 2002. Regional and progressive thinning of the cortical ribbon in Huntington's disease. Neurology 58, 695–701.
Sabuncu, M.R., Desikan, R.S., Sepulcre, J., Yeo, B.T., Liu, H., Schmansky, N.J., Reuter, M., Weiner, M.W., Buckner, R.L., Sperling, R.A., Fischl, B., Alzheimer's Disease Neuroimaging, I., 2011. The dynamics of cortical and hippocampal atrophy in Alzheimer disease. Arch. Neurol. 68, 1040–1048.
Salat, D.H., Buckner, R.L., Snyder, A.Z., Greve, D.N., Desikan, R.S., Busa, E., Morris, J.C., Dale, A.M., Fischl, B., 2004. Thinning of the cerebral cortex in aging. Cereb. Cortex 14, 721–730.
Segonne, F., Dale, A.M., Busa, E., Glessner, M., Salat, D., Hahn, H.K., Fischl, B., 2004. A hybrid approach to the skull stripping problem in MRI. Neuroimage 22, 1060–1075.
Segonne, F., Pacheco, J., Fischl, B., 2007. Geometrically accurate topology-correction of cortical surfaces using nonseparating loops. IEEE Trans. Med. Imaging 26, 518–529.
Sheikh, J.I., Yesavage, J.A., 1986. Geriatric Depression Scale (GDS): recent evidence and development of a shorter version. Clinical Gerontology: a Guide to Assessment and Intervention. The Haworth Press, New York, 165–173.
Sled, J.G., Zijdenbos, A.P., Evans, A.C., 1998. A nonparametric method for automatic correction of intensity nonuniformity in MRI data. IEEE Trans. Med. Imaging 17, 87–97.
Sowell, E.R., Peterson, B.S., Kan, E., Woods, R.P., Yoshii, J., Bansal, R., Xu, D., Zhu, H., Thompson, P.M., Toga, A.W., 2007. Sex differences in cortical thickness mapped in 176 healthy individuals between 7 and 87 years of age. Cereb. Cortex 17, 1550–1560.
Storsve, A.B., Fjell, A.M., Tamnes, C.K., Westlye, L.T., Overbye, K., Aasland, H.W., Walhovd, K.B., 2014. Differential longitudinal changes in cortical thickness, surface area and volume across the adult life span: regions of accelerating and decelerating change. J Neurosci. 34, 8488–8498.
Thambisetty, M., Wan, J., Carass, A., An, Y., Prince, J.L., Resnick, S.M., 2010. Longitudinal changes in cortical thickness associated with normal aging. Neuroimage 52, 1215–1223.
Vita, A., De Peri, L., Deste, G., Sacchetti, E., 2012. Progressive loss of cortical gray matter in schizophrenia: a meta-analysis and meta-regression of longitudinal MRI studies. Transl. Psychiatry 2, e190.
Walhovd, K.B., Westlye, L.T., Amlien, I., Espeseth, T., Reinvang, I., Raz, N., Agartz, I., Salat, D.H., Greve, D.N., Fischl, B., Dale, A.M., Fjell, A.M., 2011. Consistent neuroanatomical age-related volume differences across multiple samples. Neurobiol. Aging 32, 916–932.